CHARLES UNIVERSITY
Faculty of Science
Department of Genetics and Microbiology

Study Programme: Genetics, Molecular Biology and Virology
Specialization: Molecular Biology and Genetics of Eukaryotes

Bc. Klára Viktorinová

Study of Mammalian NudiX Enzymes and Their RNA Decapping Activity

Studium savčích NudiX enzymů a jejich aktivity na RNA čepičkách

Master's Thesis

Supervisor: Ing. Hana Macíčková Cahová, Ph.D.
Consultant: Mgr. Ondřej Nešuta, Ph.D.

Prague, 2025

Prohlašuji, že jsem závěrečnou práci vypracovala samostatně a že jsem uvedla všechny použité informační zdroje a literaturu. Tato práce ani její podstatná část nebyla předložena k získání jiného nebo stejného akademického titulu. Ke stylistickým úpravám textu byly využity nástroje umělé intelligence.

V Praze dne 7. 8. 2025 Bc. Klára Viktorinová

Acknowledgements

First, I would like to thank to my supervisor, Dr. Hana Macíčková Cahová, for the opportunity to work on my master's thesis in her group, for all the resources, and for her never-ending guidance, support, and patience during the entire project. I am also very grateful to my consultant, Dr. Ondřej Nešuta, for guiding me in the laboratory, for teaching me so much, and for supporting me, both professionally and personally. My thanks also go to Dr. Anton Škríba for the LC-MS measurements and for his help with HPLC experiments, and to Dr. Maria Bianca Mititelu for her support during protein expression and purification, as well as her overall assistance in the laboratory. Next, I would like to thank to Pål Stenmark for kindly providing the NudiX enzymes that were essential for my experiments. A special thank you to all the other members of the Hana Cahová group for their help whenever I needed it and for creating such a friendly and supportive work environment. Finally, I am deeply thankful to my loved ones for standing by me during challenging times and for never giving up on me.

Abstract (EN)

The discovery of non-canonical RNA caps such as NAD, FAD, and dinucleoside polyphosphates (Np_nNs) has expanded the known portfolio of RNA modifications. However, the physiological relevance and metabolic fate of these RNA caps remain poorly understood. NudiX hydrolases, known for cleaving nucleotide-derived substrates with polyphosphate backbones, are major candidates for hydrolyzing these non-canonical RNA caps. While some mammalian NudiX enzymes have been shown to act on some small molecules and capped RNAs, their broader substrate specificity remains largely unexplored.

This thesis systematically investigates the substrate specificity of seven selected mammalian NudiX enzymes, with a particular focus on their RNA decapping activity. The study includes expression and purification of the mouse NUDT12 enzyme, as well as the synthesis and purification of capped 6-mer RNAs, tested as potential NudiX substrates. To assess enzymatic activity, a newly optimized malachite green assay (MGA) was employed. Among the tested enzymes, HsNUDT2 was identified as the only enzyme that preferentially hydrolyzes RNA substrates over small molecules.

This work provides the first systematic comparison of RNA versus small molecule substrate specificity across multiple mammalian NudiX enzymes and validates MGA as a reliable, quantitative method for enzymatic characterization. Overall, these findings expand current knowledge of mammalian NudiX enzyme function and contribute to a deeper understanding of metabolic processing of non-canonically capped RNAs.

Keywords

Non-canonical RNA caps, dinucleoside polyphosphates, NudiX enzymes, malachite green assay

Abstrakt (CZ)

Objev nekanonických RNA čepiček, jako jsou NAD, FAD a dinukleosid polyfosfáty (Np_nNs), rozšířil portfolio známých RNA modifikací. Fyziologický význam a metabolický osud těchto RNA čepiček však zůstávají dosud nedostatečně prostudovány. NudiX hydrolasy, známé svou schopností štěpit substráty odvozené od nukleotidů s polyfosfátovou kostrou, představují hlavní kandidáty pro hydrolýzu těchto nekanonických RNA čepiček. Ačkoliv bylo prokázáno, že některé savčí NudiX enzymy působí na některé malé molekuly a čepičkované RNA, jejich širší substrátová specificita zůstává do značné míry neprozkoumána.

Tato diplomová práce systematicky studuje substrátovou specificitu sedmi vybraných savčích NudiX enzymů, s hlavním zaměřením na jejich hydrolýzu RNA čepiček. Studie zahrnuje expresi a purifikaci jednoho z enzymů, myšího NUDT12, stejně jako syntézu a purifikaci čepičkovaných hexamerních RNA, které byly následně použity jako substráty NudiX enzymů. K vyhodnocení enzymové aktivity byl použit nově optimalizovaný test s malachitovou zelení (MGA). Mezi testovanými enzymy byl HsNUDT2 jediný, který preferenčně štěpil RNA substráty před malými molekulami.

Tato práce poskytuje první systematické srovnání RNA a malých molekul jakožto substrátů pro savčí NudiX enzymy a potvrzuje, že MGA je spolehlivou a kvantifikovatelnou metodou pro enzymovou charakterizaci. Celkově tyto poznatky rozšiřují současné znalosti o funkci savčích NudiX enzymů a přispívají k hlubšímu porozumění metabolismu nekanonických RNA čepiček.

Klíčová slova

Nekanonické RNA čepičky, dinukleosid polyfosfáty, NudiX enzymy, test malachitové zeleně

Table of Contents

List of abbreviations

$[PP]_2$-$InsP_4$	bis(1,4)-diphosphoinositol tetrakisphosphate
A	adenine
ADP	adenosine diphosphate
ADPR	adenosine diphosphate ribose
AMP	adenosine monophosphate
Ap_2A	diadenosine diphosphate
Ap_2G	adenosine guanosine diphosphate
Ap_3A	diadenosine triphosphate
Ap_3G	adenosine guanosine triphosphate
Ap_4A	diadenosine tetraphosphate
Ap_4G	adenosine guanosine tetraphosphate
Ap_5A	diadenosine pentaphosphate
Ap_5G	adenosine guanosine pentaphosphate
Ap_6A	diadenosine hexaphosphate
ApaH	bis(5′-nucleosyl)-tetraphosphatase
Ap_nAs	diadenosine polyphosphates
Ap_nGs	adenosine guanosine polyphosphates
ASFV	African Swine Fever Virus
At	*Arabidopsis thaliana*
ATP	adenosine triphosphate
AUC	area under curve
C	cytosine
CMTR1	mRNA (nucleoside-2'-O-)methyltransferase 1
CMTR2	mRNA(nucleoside-2'-O)methyltransferase 2
CoA	coenzyme A
CTP	cytosine triphosphate
DCP1	mRNA decapping enzyme 1
DCP2	mRNA decapping enzyme 2
DMSO	dimethyl sulfoxide
DNA	deoxyribonucleic acid
dGTP	deoxyriboguanosine triphosphate

dNTPs	deoxyribonucleoside triphosphates
dpCoA	3'-dephospho-CoA
DTT	dithiothreitol
DXO	decapping and exoribonuclease
E. coli	*Escherichia coli*
EDTA	ethylenediaminetetraacetic acid
FAD	flavin adenine dinucleotide
G	guanine
GDP	guanosine diphosphate
GTP	guanosine triphosphate
HCV	Hepatitis C Virus
HPLC	high-pressure liquid chromatography
Hs	*Homo sapiens*
IDP	inosine diphosphate
IMAC	immobilized metal ion affinity chromatography
IPTG	isopropyl-β-D-thiogalactopyranoside
IVT	in vitro transcription
LB medium	Luria-Bertani medium
LC-MS	liquid chromatography coupled with mass spectrometry
lncRNAs	long non-coding RNAs
m^6A	6-methyladenosine
m^7G	7-methylguanosine
m^7GDP	7-methylguanosine diphosphate
m^7Gp_3A	7-methylguanosine adenosine triphosphate
MGA	malachite green assay
Mm	*Mus musculus*
mRNA	messenger RNA
NAD	nicotinamide adenine dinucleotide
NADH	reduced form of NAD
NCIN	non-canonical initiating nucleotide
NEB	New England Biolabs
NMN	nicotinamide mononucleotide
Np_nNs	dinucleoside polyphosphates

NTPs	ribonucleoside triphosphates
NudiX	nucleoside diphosphates linked to X
OD_{600}	optical density at 600 nm
PAGE	polyacrylamide gel electrophoresis
PARPs	poly(ADP-ribose) polymerases
P_i	inorganic phosphate
PPH	pyrophosphohydrolase
PP_i	pyrophosphate
PP-$InsP_5$	diphosphoinositol pentakisphosphate
ppp-RNA	5’-triphosphorylated RNA
p-RNA	5’-monophosporylated RNA
RNA	ribonucleic acid
RppH	RNA 5’-pyrophosphohydrolase
rRNA	ribosomal RNA
rSAP	recombinant shrimp alkaline phosphatase
SD	standard deviation
SDS-PAGE	sodium dodecyl sulfate polyacrylamide gel electrophoresis
SEC	size exclusion chromatography
sncRNAs	small non-coding RNAs
snoRNA	small nucleolar RNA
snRNA	small nuclear RNA
TBE	Tris-borate-EDTA
TCEP	tris(2-carboxyethyl)phosphine
TEAA	triethylammonium acetate
Tris	tris(hydroxymethyl)aminomethane
tRNA	transfer RNA
U	uracil
UDP	uridine diphosphate
UTP	uridine triphosphate
Ψ	pseudouridine

Introduction

For many years, the canonical 5′ cap structure of eukaryotic mRNAs, composed of a 7-methylguanosine (m^7G) linked by a 5′-5′ triphosphate bridge, was the only known 5’ RNA modification. This RNA cap plays a crucial role in RNA stability, nuclear export, and translation initiation. However, recent discoveries have significantly expanded this understanding with the identification of non-canonical RNA caps, including metabolites such as nicotinamide adenine dinucleotide (NAD), flavin adenine dinucleotide (FAD), coenzyme A (CoA), and dinucleoside polyphosphates (Np_nNs). These molecules can be incorporated at the 5′ end of RNA either co-transcriptionally by RNA polymerases or post-transcriptionally through other enzymatic reactions.

Despite growing evidence of their existence across different organisms and RNA types, the biological function of non-canonical RNA caps remains largely unclear. They are thought to influence RNA stability, translation efficiency, and cellular stress responses. To understand their physiological relevance, it is essential to characterize enzymes responsible for their synthesis and degradation. One group of candidate enzymes involved in the removal of these caps are NudiX hydrolases.

NudiX enzymes are a diverse superfamily of hydrolases found in all domains of life. They are characterized by a conserved NudiX motif and are capable of cleaving substrates that contain a nucleoside and a polyphosphate backbone (**nuc**leoside **di**phosphate linked to moiety **X**). While several studies have reported decapping activity for a few prokaryotic and eukaryotic NudiX enzymes, most members of this family remain poorly characterized in terms of substrate specificity, particularly RNA decapping.

This thesis addresses this knowledge gap by systematically investigating the substrate specificity of seven selected mammalian NudiX enzymes, focusing on their ability to cleave small molecules and capped RNAs. The work combines traditional analytical methods such as HPLC and PAGE with an optimized high-throughput malachite green assay to provide a comprehensive overview of NudiX enzyme activity. Through this approach, the thesis aims to expand current understanding of NudiX function and their potential role in RNA decapping.

1. Literature Review

1.1. Ribonucleic Acid

Ribonucleic acid (RNA) is a fundamental molecule found in all living organisms, playing a crucial role in protein biogenesis. Beyond its role in this process, RNA also contributes to the regulation of gene expression at the post-transcriptional level (Chen and Rajewsky, 2007) and functions as a catalytic molecule in certain cellular reactions (Westheimer, 1986). Rather than having a single purpose, RNA represents a diverse class of molecules with various structural, regulatory, and catalytic roles across all domains of life.

1.1.1. Types of RNA

Multiple types of RNA exist in cells. The three main types involved in protein biogenesis are messenger RNA (mRNA), ribosomal RNA (rRNA) and transfer RNA (tRNA), each with its own specific structure and function. mRNA serves as an intermediate in the process of gene expression. It is synthesized as a complementary copy of 2'-deoxyribonucleic acid (DNA) sequence in the nucleus during process called transcription and carries a copy of the genetic information into the cytoplasm, where it is translated into proteins on ribosomes.

The other two types – rRNA and tRNA – are also involved in the process of protein biogenesis, specifically in the mRNA translation. rRNA is a component of the translation nucleoprotein particles called ribosomes. In eukaryotic cells, four types of rRNA exist – 5S, 18S, 5.8S and 28S. The 5S, 5.8S and 28S are part of the large ribosomal subunit, while 18S is found in the small ribosomal subunit. The role of tRNA is to carry single amino acids into the ribosome during translation. Each of the 61 tRNAs recognizes a specific codon on the mRNA strand, which consists of a triplet of nucleotides, and leads to the incorporation of the correct amino acid into the growing polypeptide chain of the forming protein. The recognition of the mRNA codon is mediated through complementary base-pairing between codon on the mRNA and anticodon on the tRNA. The relationship between codons and amino acids is defined by the genetic code. Out of 64 possible codons, 61 encoding amino acids are recognized by tRNAs, while the remaining three function as stop codons and signal the termination of translation. Since multiple codons can encode the same amino acid, the genetic code is described as degenerate (Alberts *et al.*, 2015).

In addition, many other types of RNA are present in cells (Figure 1). Collectively, these are referred to as regulatory or non-coding RNAs. These RNAs are primarily classified based on their size. RNAs shorter than 200 nucleotides are considered small non-coding RNAs (sncRNAs), while RNAs longer than 200 nucleotides are considered long non-coding RNAs (lncRNAs). Among sncRNAs, small silencing RNAs play a key role in gene regulation, usually by reducing the levels of their target mRNAs (Ghildiyal and Zamore, 2009). The group of small silencing RNAs includes micro RNAs which typically bind to mRNA and target it for degradation or inhibit its translation (Carrington and Ambros, 2003) and double-stranded small silencing RNAs which are processed into single-stranded small interfering RNAs and regulate gene expression at the post-transcriptional level through RNA interference (Fire *et al.*, 1998). Even though miRNA and siRNA have a similar function, they differ in their origin, structure, processing and specificity. miRNAs are endogenously encoded RNAs derived from imperfectly base-paired hairpin precursors and often regulate multiple mRNAs, whereas siRNAs are typically of exogenous origin and exhibit high specificity toward a single mRNA target (Carthew and Sontheimer, 2009).

Furthermore, small nuclear RNA (snRNA) and small nucleolar RNA (snoRNA) also belong to the group of sncRNAs. snRNAs are components of the spliceosome, a ribonucleoprotein complex that removes introns from pre-mRNA in a process called splicing (Chow *et al.*, 1977). Splicing is essential for producing mature, translatable mRNA. In contrast to snRNAs, snoRNAs do not participate in splicing but instead guide chemical modifications of other types of RNA.

While sncRNAs typically function through base-pairing interactions, lncRNAs contribute to gene regulation through more structurally diverse and often less sequence-specific mechanisms. They are involved in processes including chromatin remodeling, and modulation of mRNA stability. Some lncRNAs act as scaffolds for protein complexes, while others regulate gene expression by directly interacting with DNA, RNA, or proteins (Ponting, Oliver and Reik, 2009).

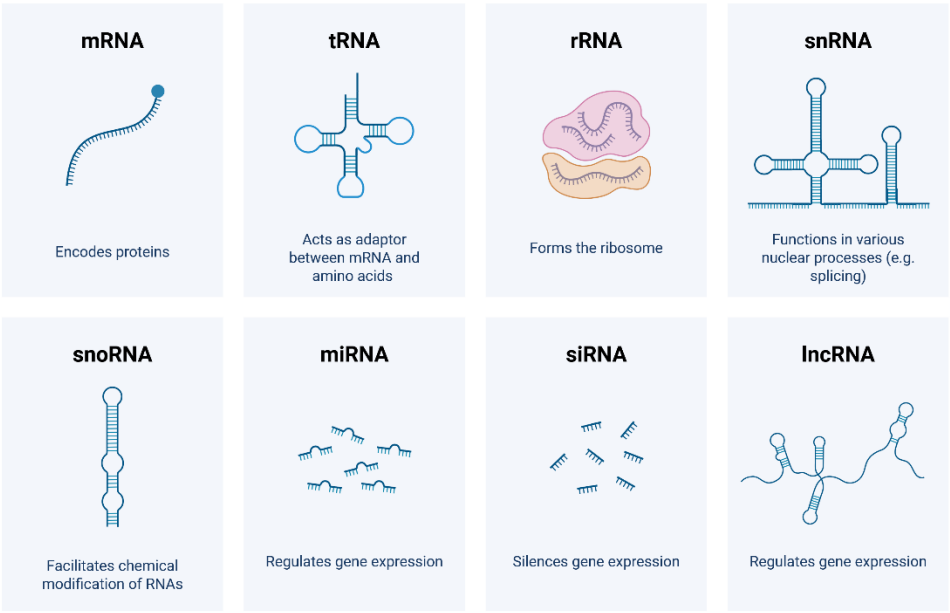

***Figure 1**: Types of RNA occurring in cells, their structure, and function. Created in https://BioRender.com.*

1.1.2. Structure of RNA

RNA is usually a single-stranded polynucleotide composed of individual nucleotides. Each nucleotide consists of a ribose sugar, a phosphate group, and one of four nucleobases – adenine (A), guanine (G), cytosine (C), or uracil (U) (Figure 2). The ribose and phosphate groups are linked by phosphodiester bonds, forming the RNA backbone, while nucleobases are attached to the ribose by N-glycosidic bonds. The specific sequence of nucleotides is called primary structure of RNA and is essential for encoding genetic information. RNA is oriented from the 5' to 3' end, starting with a free phosphate group at the 5′ ribose position of the first nucleotide and ending with a free hydroxyl group at the 3′ ribose position of the last nucleotide. This 5′ to 3′ polarity is critical for RNA synthesis and degradation. Although RNA is single-stranded, it often folds into secondary structures, such as hairpins and internal loops, through intramolecular base-pairing, which can affect its stability, and biological activity (Alberts *et al.*, 2015).

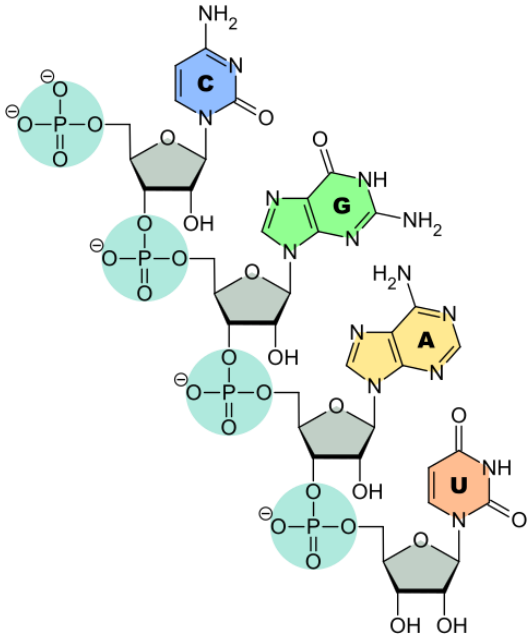

***Figure 2**: Primary structure of RNA fragment, containing ribose, phosphate, and all four types of nucleobases – adenine (A), guanine (G), cytosine (C) and uracil (U) (Source: Wikimedia Commons).*

In addition to its primary and secondary structures, RNA can have several chemical modifications that influence its stability, function, and fate in the cell. RNA modifications represent a rapidly expanding field of study and have been identified in all types of RNAs across all three domains of life. To this date, more than 170 RNA modifications have been discovered (Cappannini *et al.*, 2024). Among these, tRNA has been recognized as the most post-transcriptionally modified type of RNA with more than 100 known modifications (McCown *et al.*, 2020). These modifications are present at internal positions, as well as at the 5' or 3' ends of RNA. In some RNAs, specific modifications are essential for proper function. Moreover, modifications can affect RNA stability, and their absence or misregulation has been linked to various diseases.

Many RNA modifications are present at internal positions, where nucleobases are chemically modified, most commonly through methylation, acetylation, or isomerization. These modifications are not equally distributed among the four nucleotides. The most frequently modified nucleoside is uridine, from which the first known RNA modification, pseudouridine (Ψ), is derived. Ψ, an isomer of uridine where the N-glycosidic bond is replaced by a C-C bond, is also the most abundant internal RNA modification (Cohn and Volkin, 1951). Adenosine is another highly modified base. Among its modifications, N6-methyladenosine (m^6A) is now

recognized as one of the most prevalent internal RNA modifications. The presence of m^6A has been linked to various diseases, including different types of cancer (Deng *et al.*, 2023). While cytidine and guanosine also undergo internal chemical modifications, such as 5-methylcytidine, N4-acetylcytidine, and 7-methylguanosine (m^7G), current research has predominantly focused on uridine and adenosine derivatives because of their higher abundance (Franco and Koutmou, 2022).

In addition to internal modifications, chemical modifications also occur at the 5′ and 3′ ends of RNA. These terminal modifications are important for RNA stability and processing. At the 3′ end, the most common modification is the addition of a poly(A) tail. The 5′ end is often modified by the addition of a cap structure. RNA caps are essential for RNA protection and function. They are the main topic of this thesis and will be the focus of the following sections.

1.2. RNA Caps

5’ RNA modifications, commonly known as 5’ RNA caps, are found at the 5’ end of various RNA molecules. The most abundant and well-studied cap is N^7-methylguanosine (m^7G) present on eukaryotic mRNA (Potužník and Cahová, 2024). Since m^7G was the only known RNA cap for a long time, it is known as the canonical cap. While m^7G functions as a cap in eukaryotic mRNA, prokaryotic RNA has been believed for long time to contain only a triphosphate group instead. Recently, several other 5’ RNA caps, such as nicotinamide adenine dinucleotide (NAD) (Cahová *et al.*, 2015), coenzyme A (CoA) (Kowtoniuk *et al.*, 2009), flavin adenine dinucleotide (FAD) (Wang *et al.*, 2019) or dinucleoside polyphosphate (Np_nN) (Hudeček *et al.*, 2020) have been discovered. Because these caps are relatively novel and have only been studied in recent years, they are called non-canonical caps. The RNA cap is attached to the RNA backbone by a 5’ to 5’ triphosphate linkage. This bond cannot be cleaved by 5’ to 3’ exonucleases, therefore it may protect RNA from degradation. The following sections will focus on chemical structures that can function as 5′ RNA caps, describing both canonical and non-canonical caps.

1.2.1. Canonical RNA Cap

The canonical m^7G cap is present on all eukaryotic mRNAs and is highly conserved across species. Its primary role is to enhance mRNA stability by protecting the eukaryotic 5′ end from degradation by 5′ to 3′ exonucleases (Furuichi, Lafiandra and Shatkin, 1977). Additionally,

the cap is essential for efficient translation initiation. It is specifically recognized by the eukaryotic translation initiation factor 4E, which is part of the larger eukaryotic translation initiation factor 4F complex responsible for recruiting the ribosome to the mRNA (Muthukrishnan *et al.*, 1975).

The m^7G capping takes place co-transcriptionally in the nucleus, usually after the first 25-30 nucleotides of the nascent transcript have been synthesized. Three different enzymes are involved in the capping process: RNA triphosphatase, RNA guanylyltransferase and guanine-N^7methyltransferase. RNA triphosphatase removes the γ-phosphate from the 5' triphosphate. RNA guanylyltransferase then adds a guanosine monophosphate to the 5' diphosphate. Finally, the guanine-N^7methyltransferase methylates the N^7 position of the guanine (Shatkin and Manley, 2000; Ramanathan *et al.*, 2016). In humans, the RNA triphosphatase and RNA guanylyltransferase activities are performed by a single enzyme known as the human capping enzyme (Yamada-Okabe *et al.*, 1998). The resulting cap structure is known as cap 0 (Figure 3).

The cap 0 can be modified further. In higher eukaryotes, the 2'-O-ribose of the first transcribed nucleotide, or of both the first and the second nucleotides, can be methylated. Cap 1 contains a methyl group on the 2'-O-ribose of the first nucleotide while cap 2 contains methyl group on the 2'O-ribose of both the first and the second nucleotides (Figure 3). These methylations are catalyzed by two enzymes – mRNA (nucleoside-2'-O-)methyltransferase 1 (CMTR1) and mRNA (nucleoside-2'-O)methyltransferase 2 (CMTR2) (Werner *et al.*, 2011).

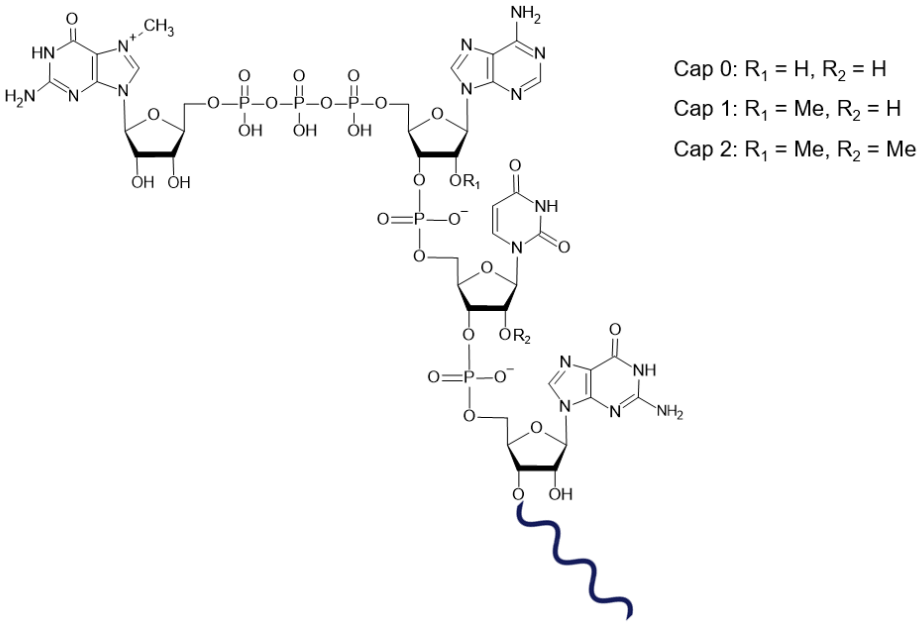

***Figure 3**: Structure of the canonical mRNA m⁷Gp₃A cap. Cap 0 consists of an m⁷G connected via a 5'–5' triphosphate bridge to the first transcribed nucleotide, without 2'-O-methylation. Cap 1 includes an additional methyl group (Me) at the 2'-O position of the ribose on the first nucleotide. Cap 2 has methylation at the 2'-O position on both the first and the second nucleotides.*

1.2.2. Cofactor RNA Caps

Cofactors such as NAD, FAD, and CoA are abundant molecules recognized for their roles in enzymatic reactions. NAD and FAD act as redox cofactors, carrying electrons in metabolic pathways such as glycolysis and β-oxidation. Additionally, NAD serves as a cosubstrate for enzymes like sirtuins (Avalos, Bever and Wolberger, 2005) and poly(ADP-ribose) polymerases (PARPs) (Langelier *et al.*, 2018). CoA primarily functions as a carrier of acyl groups.

The first identified cofactor-derived RNA cap was NAD (Figure 4A). In 2009, the NAD-linked RNA was described using liquid chromatography coupled with mass spectrometry (LC-MS) (Chen *et al.*, 2009). In that study, they identified the NAD-linked RNA in *Escherichia coli* (*E. coli*) and *Streptomyces venezuelae*, demonstrating that NAD can serve as a 5' RNA modification, with an abundance of approximately 3000 copies per cell.

Six years later, NAD-linked RNA in bacteria was further characterized using a method called chemo-enzymatic capture combined with next-generation sequencing (NAD captureSeq)

(Cahová *et al.*, 2015). The approach of this method relies on a series of chemical reactions that selectively bind NAD-capped RNA to an affinity matrix. The captured RNA is then sequenced, allowing for its identification.

To date, NAD captureSeq and its modified versions have been applied not only in bacteria but also in archaea (Gomes-Filho *et al.*, 2023), yeast (Walters *et al.*, 2017), plants (Wang *et al.*, 2019) and mammals (Jiao *et al.*, 2017), revealing that NAD functions as a cap in both prokaryotes and eukaryotes. Unlike canonical RNA capping, which occurs post-transcriptionally, NAD acts as a non-canonical initiating nucleotide (NCIN) during transcription initiation by RNA polymerases (Bird *et al.*, 2016). Once transcription is complete, NAD remains covalently attached to the 5' end of RNA, forming the NAD-capped RNA. However, the biological roles of NAD-capped RNA can vary across organisms.

In bacteria, the cap is found on sncRNAs as well as on sncRNA-like 5'-terminal fragments of mRNAs (Cahová *et al.*, 2015; Frindert *et al.*, 2018). NAD in bacterial RNA shows functional similarities to the m^7G cap in eukaryotic RNA. It stabilizes the RNA and protects it against degradation by RNA pyrophosphohydrolase (RppH) and ribonucleases. Furthermore, NAD cap in bacteria regulates RNA turnover through NudC-mediated decapping. NudC is a decapping enzyme that specifically recognizes NAD-capped RNAs and removes the NAD, converting the 5′ end into a monophosphate, which then can be degraded by exonucleases (Höfer *et al.*, 2016). Recent studies have shown that NAD-RNA plays a crucial role during *E. coli* infection by T4 bacteriophage (Wolfram-Schauerte *et al.*, 2023). The viral ADP-ribosyltransferase, ModB, can attach NAD-RNA to host proteins. Inactivation of ModB slows down the lytic cycle of the T4 bacteriophage.

In yeast, NAD caps are found mostly on mitochondrial and nuclear mRNAs. RNA polymerase II initiates NAD-RNA transcription from promoters that differ from those used for m^7G-capped RNA, often resulting in incomplete transcripts. As a consequence, NAD-RNAs are usually shorter than m^7G-capped RNAs (Zhang *et al.*, 2020). While NudC decaps NAD-RNA in bacteria, Npy1 decaps the NAD-RNA in yeast. Importantly, Npy1 is specific for NAD-RNA and does not decap the canonical m^7G-capped RNA. In mammals, the NAD cap has probably different role. Instead of stabilizing RNA, it can serve as a marker for degradation (Jiao *et al.*, 2017). Despite the fact that NAD-RNA has been intensively studied in the last decade, its role in living cells remains mostly unexplored.

Moreover, during HIV-1 infection of human cells, the amount of NAD cap was significantly reduced on specific host snRNAs and snoRNAs. The NAD cap on U1 snRNA affects HIV replication by destabilizing the U1–HIV pre-mRNA duplex (Benoni *et al.*, 2022).

Another cofactor that can function as an RNA cap is FAD. FAD, like NAD, can serve as NCIN during transcription initiation (Huang, 2003) (Figure 4B). This cap has been detected at the 5' end of RNA using LC-MS in both viral and cellular transcripts (Wang *et al.*, 2019). In 2023, the study on Hepatitis C virus (HCV) revealed that approximately 75% of HCV transcripts are FAD-capped (Sherwood *et al.*, 2023). The FAD cap in HCV protects viral RNA from innate immune recognition, although it does not stabilize the HCV RNA.

Coenzyme A (CoA) is another coenzyme that was detected at the 5' end of various RNA (Figure 4C). In 2009, the CoA RNA cap and its derivatives – 3'-dephospho-CoA (dpCoA), succinyl-dephospho-CoA and acetyl-dephospho-CoA – were identified at the 5' end of *E. coli* and *Streptomyces venezuelae* (Kowtoniuk *et al.*, 2009). Later, the dpCoA cap was detected in a small fraction of *Staphylococcus aureus* RNA, with an abundance of 0.03-0.04% (Löcherer *et al.*, 2022). Like NAD and FAD, dpCoA can serve as NCIN during in vitro transcription (Huang, 2003). However, unlike NAD and FAD, dpCoA can be added also post-transcriptionally. The phosphopantetheine adenylyltransferase can accept RNA transcripts as substrates to form CoA-RNA, although the reaction was not very efficient and only small portion of 5'-triphoshorylated RNA (ppp-RNA) was capped with CoA (Sapkota *et al.*, 2024).

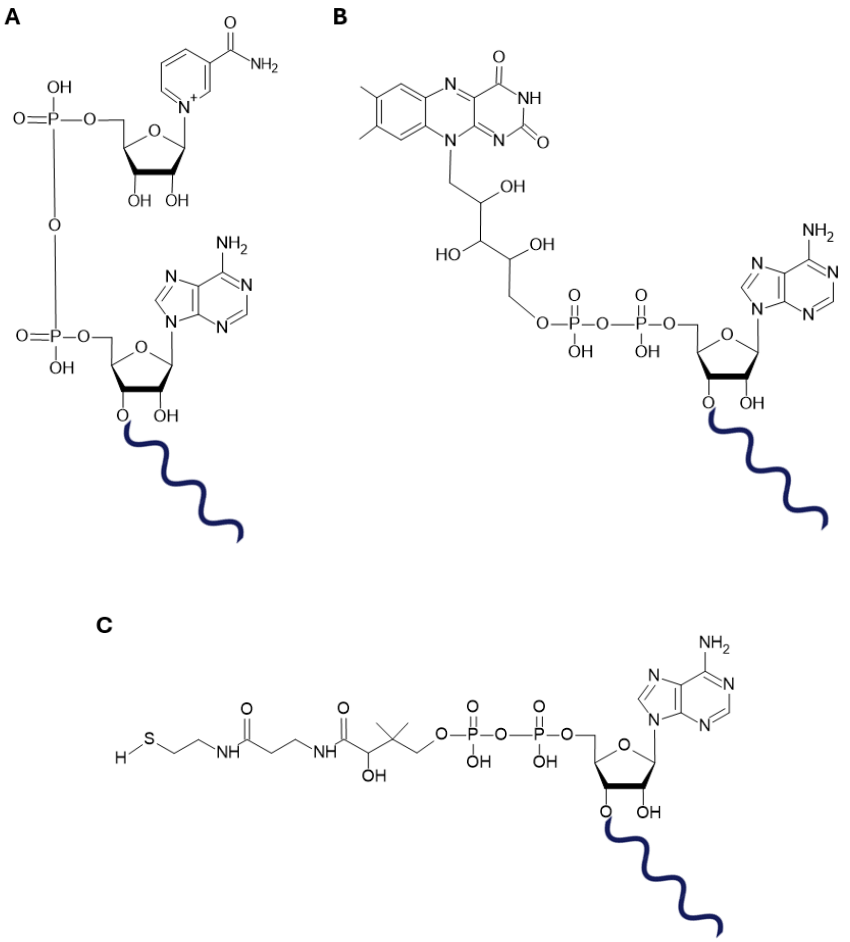

***Figure 4**: Structure of **(A)** NAD-RNA, **(B)** FAD-RNA, and **(C)** CoA-RNA.*

1.2.3. Adenosine Diphosphate Ribose Cap

For a long time, adenosine diphosphate ribose (ADPR) was considered exclusively a protein modification, targeting specific amino acids such as glutamate, aspartate, and serine (Tashiro *et al.*, 2023). However, recent studies have identified ADPR as a nucleic acid modification which plays a role in the DNA damage response and can occur at the 5' end of RNA (Weixler *et al.*, 2021) (Figure 5). ADP-ribosylation is a transfer of ADPR from the NAD cofactor to target molecules (Chambon, Weill and Mandel, 1963). The enzymes catalyzing the ADP-ribosylation in proteins are called poly(ADP-ribose) polymerases (PARPs) (Schreiber *et al.*, 2006). While some PARPs, such as PARP1 and PARP2, primarily catalyze poly-ADP-ribosylation (PARylation) by adding multiple ADPR on the acceptor molecule, other PARPs, particularly PARP10, PARP12, and PARP14, function mainly as mono-ADP-ribosyltransferases, catalyzing mono-ADP-ribosylation (MARylation).

In addition to PARPs, tRNA 2'-phosphotransferase 1 (TRPT1) catalyzes the ADP-ribosylation of the 5'-phosphate of single-stranded RNA (Munir, Banerjee and Shuman, 2018).

In 2022, the RNA MARylation was described in human cells, establishing ADPR as a novel non-canonical RNA cap. Moreover, the study showed that the level of ADPR-RNA increases under stress conditions (Weixler, Feijs and Zaja, 2022).

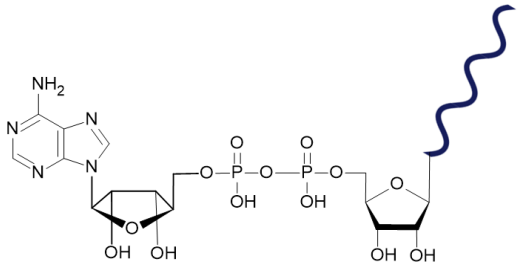

***Figure 5**: Structure of ADPR-RNA.*

1.2.4. Dinucleoside Polyphosphate Caps

Another class of non-canonical RNA caps are dinucleoside polyphosphates (Np_nNs), nucleotide-derived molecules long known for their signaling roles in the cell. Np_nNs consist of two nucleosides linked through a 5'-5' polyphosphate bridge containing two to six phosphate groups. While both purines and pyrimidines can form Np_nNs, purine-containing variants are more common.

Before their discovery as RNA caps, Np_nNs were primarily studied as small molecules. They were first identified over 50 years ago during studies of lysyl-tRNA synthetase (Zamecnik *et al.*, 1966). Back then, two key Np_nNs – diadenosine tetraphosphate (Ap_4A) and diadenosine triphosphate (Ap_3A) – were discovered. Aminoacyl-tRNA synthetases were later found to produce these molecules as by-products during aminoacylation of tRNAs. For example, lysyl-tRNA synthetase catalyzes the formation of Ap_4A by transferring lysine to tRNA, under certain conditions the adenine monophosphate (AMP) moiety is instead transferred to the α-phosphate of adenosine triphosphate (ATP), generating Ap_4A with a characteristic 5'-5' tetraphosphate bridge (Hilderman and Ortwerth, 1987). Another group of enzymes capable of forming Np_nNs are ubiquitin ligases. In this case, the reaction is linked to the ATP-dependent

activation of ubiquitin. Under stress conditions, ubiquitin-activating enzyme E1 can transfer the AMP of one ATP to a second ATP molecule, forming Ap_4A (Götz *et al.*, 2019).

Np_nNs have been detected both extracellularly and intracellularly. Extracellular Np_nNs can function as neurotransmitters, modulating synaptic activity and neuronal communication (Miras-Portugal, Gualix and Pintor, 1998). Intracellularly, Np_nNs are involved in various cellular processes, including the stress response. However, even today their role within the cells is poorly understood. The intracellular concentration of diadenosine polyphosphates (Ap_nAs) in connection with stress was first studied in bacteria. In *Salmonella typhimurium*, the concentration of Ap_nAs increases under heat shock or oxidative stress (Lee, Bochner and Ames, 1983). Because of this stress-related role, these molecules are often called alarmones (Varshavsky, 1983).

In eukaryotes, Ap_nAs are implicated in cell signaling, such as regulating ATP-sensitive K^+ channels by promoting their opening or inhibition. (Kisselev *et al.*, 1998). Moreover, the intracellular concentration of Ap_4A correlates with the proliferation rate of mammalian cells. Specifically, the more the cell is proliferating the higher its concentration of Ap_4A is (Rapaport and Zamecnik, 1976). Ap_4A also plays a role in immune response (Yu *et al.*, 2019) or influences enzymes involved in purine metabolism (Giammarinaro *et al.*, 2022). Not only Ap_nAs but also adenosine guanosine polyphosphates (Ap_nGs) are present in human cells, particularly in human platelets, where they act as growth factors (Schlüter *et al.*, 1998).

In 2020, it was demonstrated that dinucleoside polyphosphates (Np_nNs) can also be present at the 5' terminus of RNA (Figure 6). The group of Hana Cahová showed that Np_nNs can act as NCIN during transcription, as they are accepted in vitro by two types of RNA polymerases – T7 RNA polymerase and *E. coli* RNA polymerase. Using LC-MS, they detected Np_nN-capped RNAs in *E. coli*, identifying nine previously unknown bacterial RNA caps in the short RNA fraction – including Ap_3A, m^6Ap_3A, Ap_3G, m^7Gp_4Gm, Ap_5A, mAp_5G, mAp_4G, mAp_5A, and $2mAp_5G$ (Hudeček *et al.*, 2020). Concurrently, the group of Joel G. Belasco independently identified Ap_4N (including Ap_4A, Ap_4G, Ap_4C, and Ap_4U) as a 5′ RNA cap in *E. coli*, further supporting the presence of Np_nN modifications in bacterial RNA. (Luciano, Levenson-Palmer and Belasco, 2019).

Recently, Np_nN-RNA, specifically Ap_4A-RNA, was also detected in two mammalian cell lines – human embryonic kidney cells (HEK293T) and rat basophilic leukemia cells (RBL-2H3) – using LC-MS (Potužník *et al.*, 2023). Ap_4A-RNA was discovered in the long fraction of RNA, but Ap_4A-mRNA was not translated into proteins, suggesting a different role of this cap.

To date, two types of Np_nN-RNA formation have been described. The first is the above-mentioned co-transcriptional capping by RNA polymerases. Secondly, the post-transcriptional formation of Np_nN cap by *E. coli* lysyl-tRNA synthetase LysU in the presence of ATP and lysine was reported. (Luciano, Levenson-Palmer and Belasco, 2019). However, this mechanism has not been confirmed in our laboratory and all the experiments employing either bacterial or human tRNA synthetases never led to RNA capping.

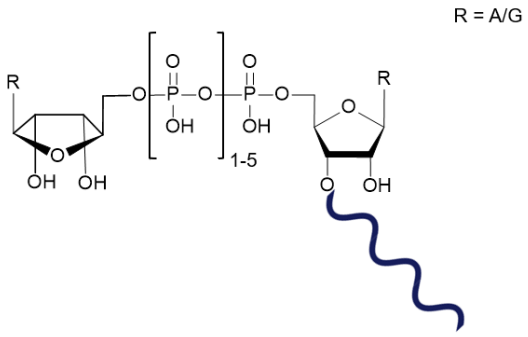

***Figure 6**: Structure of Np_nN-RNA.*

1.3. RNA Decapping Enzymes

RNA molecules which are no longer needed must be selectively removed to prevent their accumulation and to maintain cellular homeostasis. To achieve this, cells have evolved efficient mechanisms to recognize and degrade unnecessary or damaged transcripts. A crucial step in this regulatory process is the removal of the 5′ cap structure by RNA decapping enzymes. Several enzyme families have been identified to have this type of enzymatic activity, including the NudiX hydrolase superfamily, the DXO family, and the ApaH-like phosphatases (Kramer and McLennan, 2019). While these enzymes were initially studied for their role in removing

canonical m^7G cap, it has become clear that many of them can also recognize and hydrolyze non-canonical RNA caps such as NAD, FAD, CoA, or Np_nNs.

1.3.1. NudiX Hydrolase Superfamily

NudiX hydrolases are found across all domains of life, from viruses to humans. This group of enzymes is very diverse and mostly composed of pyrophosphohydrolases unified by the NudiX motif, which is conserved across all members. The NudiX motif, (Gx5Ex5[UA]xREx2EExGU), contains 23 conserved amino acids where U represents aliphatic hydrophobic amino acid and X represents any amino acid (McLennan, 2006). However, even this motif can slightly differ in some hydrolases.

The general substrates for NudiX hydrolases are **nu**cleoside **di**phosphates linked to another moiety **X** (Bessman, Frick and O'handley, 1996), which is also the origin of the enzyme family's name. These enzymes are capable of cleaving deoxyribonucleoside triphosphates, their oxidized forms, Np_nNs, 5' RNA caps etc. The catalytic activity of NudiX enzymes is dependent on Mg^{2+} ions as cofactors. The catalytic site of NudiX enzymes forms loop-helix-loop structure and usually contains two or three glutamate residues for the ion coordination (She *et al.*, 2005). In some cases, not only Mg^{2+} but also other cations, such as Mn^{2+} or Zn^{2+}, can act as cofactors.

1.3.1.1. Viral NudiX Hydrolases

NudiX hydrolases are also present in many types of viruses. Some viruses encode a complete NudiX enzyme, while others encode NudiX-like domains as part of multifunctional proteins. Among viruses, large DNA viruses are the most extensively studied in the context of decapping enzymes. Vaccinia Virus, Mimivirus and African Swine Fever Virus (ASFV) all contain genes for NudiX hydrolyses in their genome.

For example, the Vaccinia virus D10 NudiX protein is involved in mRNA turnover of both host and viral mRNAs by cleaving canonical 5' cap and producing 7-methylguanosine 5'-diphosphate (m^7GDP) as a product (Parrish, Resch and Moss, 2007). Another Vaccinia virus protein D9 also decaps both host and viral RNA (Maciej and Chakrabarti, 2022).

Mimivirus also encodes two NudiX enzymes – L375 and L543 (Kago and Parrishid, 2021). L543 has not been functionally characterized and therefore there is no evidence about RNA decapping. L375 is similar to eukaryotic mRNA decapping enzyme 2 (DCP2). It possesses

mRNA decapping activity and releases m^7GDP as a product. This enzyme uses specifically m^7G capped RNA as a substrate and does not cleave unmethylated RNAs.

ASFV decapping protein has also the NudiX motif and is capable of mRNA decapping in vitro (Quintas *et al.*, 2017). Overexpression of this protein in infected cells resulted in decreased levels of cellular and viral RNAs indicating that this enzyme tends to target both cellular and viral mRNA caps.

1.3.1.2. Bacterial NudiX Hydrolases

In bacteria, the NudiX hydrolyses play a crucial role in RNA turnover and stability. These enzymes are widely distributed among prokaryotes. However, they have been most extensively studied in *E. coli* where overall 13 NudiX-encoding genes were described. The first characterized NudiX was MutT protein (Bessman, Frick and O'handley, 1996). This protein contains conserved NudiX motif and has enzymatic activity not only against canonical ribonucleoside triphosphates (NTPs) and deoxyribonucleotide triphosphates (dNTPs) but also against 8-oxo-dGTP – a product of reactive oxygen species (McLennan, 1999). The enzymatic activity against 8-oxo-dGTP prevents 8-oxo-GTP from being incorporated into DNA and creating transversion mutation – point mutation in which a purine base is replaced by a pyrimidine, or pyrimidine base by a purine, potentially leading to harmful genetic changes (Maki and Sekiguchi, 1992).

Another example of bacterial enzyme containing the conserved NudiX motif is RppH which removes pyrophosphate from the 5' end of prokaryotic RNA and turns triphosphatate into monophosphate. This enzymatic activity is usually followed by RNAse E-mediated RNA degradation (Deana, Celesnik and Belasco, 2008).

Another bacterial NudiX enzyme, NudC, is responsible for removing the NAD cap from bacterial RNA. NudC hydrolyzes the pyrophosphate bond, producing nicotinamide mononucleotide (NMN) and 5'-monophosphate RNA (p-RNA) (Cahová *et al.*, 2015; Höfer *et al.*, 2016). NudC is a NAD(H) pyrophosphohydrolase and can also cleave free NAD and reduced form of NAD (NADH). However, in vitro studies show that NudC preferentially targets NAD-RNA over free NAD (Höfer *et al.*, 2016).

1.3.1.3. Plant NudiX Hydrolases

The group of plant NudiX hydrolases is very diverse with enzymes localized in various cellular compartments – cytosol, mitochondria and chloroplasts – which contributes to a wide range of their functions. In *Arabidopsis thaliana* (At), in total 28 NudiX-encoding genes have been identified (Yoshimura and Shigeoka, 2014). Several of them have roles in RNA metabolism, particularly RNA decapping. The enzyme AtDCP2 is a canonical RNA decapping enzyme which removes the m^7G modification from the 5' end of mRNA and releasing m^7GDP and p-RNA as products (Xu *et al.*, 2006). In addition, AtNUDT6 and AtNUDT7 are cytosolic NudiX enzymes which can cleave Np_nN-RNAs. Furthermore, the chloroplastic AtNUDT27 is a strong RNA decapping enzyme with the ability to cleave 5' caps such as m^7G, NAD, NADH, Np_nNs, CoA and ADPR in vitro and chloroplastic AtNUDT19 is highly specific toward NADH and NADH-RNA (Mititelu *et al.*, 2023).

1.3.1.4. Mammalian NudiX Hydrolases

The number of NudiX-encoding genes may vary across mammals. In human cells, 24 NudiX-encoding genes have been identified, containing 22 canonical genes and two pseudogenes (McLennan, 2006). As in other organisms, NudiX enzymes are redundant, which means that more enzymes show similar substrate specificity (Table 1). For example, NUDT1 (MTH1) and NUDT15 (MTH2) are both 8-oxo-GTPases, functionally analogous to bacterial MutT. However, studies have shown that only MTH1 is biologically relevant 8-oxo-GTPase (Carter *et al.*, 2015). Another related enzyme, NUDT18, is structurally similar to MTH1 and MTH2 and displays overlapping substrate specificity. NUDT18 in comparison to MTH1 and MTH2 is more active toward nucleoside diphosphates and their oxidized forms, rather than nucleoside triphosphates (Takagi *et al.*, 2012). Among these enzymes, only MTH2 has been reported to hydrolyze the monomethylated mRNA cap (Song, Bail and Kiledjian, 2013).

Another example of structurally related NudiX enzymes include NUDT5 and NUDT14, both being able to hydrolyze ADPR and NADH and being located in cytoplasm (Carreras-Puigvert *et al.*, 2017). On the other hand, some of the NudiX enzymes exhibit similar substrate specificity despite their different structures. For instance, NUDT2 and NUDT3 cluster in different groups within the NudiX superfamily based on their amino acid sequence. They also exhibit different folding structures (Carreras-Puigvert *et al.*, 2017). However, both enzymes preferentially

cleave Ap_nAs in vitro (Carreras-Puigvert *et al.*, 2017). NUDT3 also hydrolyzes the canonical m^7G cap in cells and through stability of subset mRNAs modulates the cell migration (Grudzien-Nogalska *et al.*, 2016). NUDT2 is known to hydrolyze Ap_4A-RNA in mammalian cells (Potužník *et al.*, 2023).

One of the most extensively studied mammalian NudiX enzymes is NUDT20, commonly known as DCP2. DCP2 is the canonical decapping enzyme in eukaryotes. It works in a complex with its activator, mRNA-decapping enzyme 1 (DCP1), competing with translation initiation factor eIF4F complex for access to the canonical m^7G mRNA cap. The DCP2-DCP1 complex navigates mRNA to P-bodies where the mRNA is translationally repressed or even degraded by nucleases (Sheth and Parker, 2003).

In addition to above-mentioned enzymes, several other NudiX enzymes demonstrate RNA decapping activity. NUDT16 hydrolyzes not only the canonical m^7G cap, but also NAD-RNA, FAD-RNA, and CoA-RNA in vitro (Sharma *et al.*, 2020). NUDT12, initially characterized for its activity against NAD and NADH, was later shown to hydrolyze NAD-capped RNA, both in vitro and in living cells (Grudzien-Nogalska *et al.*, 2019).

Table 1*: List of mammalians NudiX enzymes and their known substrates. The core of this table is based on McLennan (2006), with additional information incorporated from more recent studies. Specific references for additions are indicated directly in the table.*

NudiX enzyme	Substrates	References
NUDT1 (MTH1)	8-oxo-(d)GTP, 8-oxo-(d)ATP, 2-oxo-(d)ATP	---
NUDT2	Np_nN (n≥4), CoA-RNA, FAD-RNA, Ap_4A-RNA, m^7G-RNA	(Potužník *et al.*, 2023) (Sharma *et al.*, 2020)
NUDT3	Ap_5A, Ap_6A, PP-$InsP_5$, $[PP]_2$-$InsP_4$, m^7G-RNA	(Sharma *et al.*, 2020)
NUDT4	Ap_5A, Ap_6A, PP-$InsP_5$, $[PP]_2$-$InsP_4$	---
NUDT5	ADP-sugars, 8-oxo-(d)GDP, β-NADH	(Carreras-Puigvert *et al.*, 2017)
NUDT6	NAD, NADH, ADPR, FAD	(Debar *et al.*, 2023)
NUDT7	CoA and derivates, CoA-RNA	(Sharma *et al.*, 2020)
NUDT8	CoA and derivates, CoA-RNA	(Kerr *et al.*, 2019) (Sharma *et al.*, 2020)
NUDT9	NAD, ADPR, IDP ribose, NADH, FAD,	(Debar *et al.*, 2023)
NUDT10	Ap_5A, Ap_6A, PP-$InsP_5$, $[PP]_2$-$InsP_4$	---

NudiX enzyme	Substrates	References
NUDT11	Ap_5A, Ap_6A, PP-$InsP_5$, $[PP]_2$-$InsP_4$	---
NUDT12	NADH, NAD, Ap_2A, FAD, ADPR, Ap_3A, m^7G-RNA, NAD-RNA, CoA-RNA	(Sharma *et al.*, 2020)
NUDT13	NADH, Ap_2A	---
NUDT14	ADP-sugars, GDP-glucose, UDP-glucose, NADH	(Heyen *et al.*, 2009) (Carreras-Puigvert *et al.*, 2017)
NUDT15 (MTH2)	8-oxo-dGTP, dNTP, GTP, 6-thio-GTP, m^7G-RNA, CoA-RNA	(Carreras-Puigvert *et al.*, 2017) (Sharma *et al.*, 2020)
NUDT16	m^7G-RNA (snoRNAs), NAD-RNA, FAD-RNA, CoA-RNA	(Sharma *et al.*, 2020)
NUDT17	m^7G-RNA	(Sharma *et al.*, 2020)
NUDT18	8-oxo-GDP, 8-oxo-dGDP, 8-oxo-GTP	(Carreras-Puigvert *et al.*, 2017)
NUDT19	CoA and derivatives, CoA-RNA, m^7G-RNA	(Shumar *et al.*, 2018) (Sharma *et al.*, 2020)
NUDT20 (DCP2)	m^7G-RNA	---
NUDT21	unknown	---
NUDT22	UDP-glucose, UDP-galactose	(Carter *et al.*, 2018)

1.3.2. DXO Family

Decapping and exoribonuclease (DXO) family plays critical role in maintaining mRNA integrity by recognizing and removing aberrant 5′ caps, thereby preventing the translation of defective transcripts. All enzymes from DXO family contain conserved motifs within the active site composed of six amino acid residues that are essential for the catalytic function. These residues create a specialized environment capable of coordinating divalent cations, such as Mg^{2+}, which are critical for enzymatic activity. The motif helps the substrate recognition by stabilizing interactions with the 5' end of RNA, including the cap structure or monophosphate groups (Jiao *et al.*, 2013).

In yeast, Rai1 is a well-characterized member of the DXO family, containing a conserved DXO domain which specifically targets aberrantly capped RNAs, such as those with unmethylated caps or 5′ triphosphate groups, which often accumulate under nutrient starvation conditions. By decapping these defective transcripts, Rai1 acts as a regulatory enzyme controlling mRNA translation during cellular stress (Jiao *et al.*, 2010). In addition to its decapping activity, Rai1 also exhibits pyrophosphohydrolase (PPH) activity, generating p-RNAs that are subsequently

degraded by 5′–3′ exoribonucleases (Xiang *et al.*, 2009). Another yeast enzyme, Dxo1, is a Rai1 paralog which also belongs to DXO family. Dxo1 has 5'-3' exonuclease activity and compared to other DXO enzymes has reduced RNA decapping activity. Dxo1 plays a crucial role in rRNA processing and maturation (Hurtig and Van Hoof, 2022).

Mammalian DXO is primarily involved in the quality control of mRNAs, targeting transcripts with defects in capping, splicing, or polyadenylation (Jiao *et al.*, 2013). This enzyme also possesses PPH and 5'-3' exoribonuclease activity. Additionally, mammalian DXO can also hydrolyze the NAD-capped RNA (Jiao *et al.*, 2017). In contrast to NudiX enzymes, DXO cleaves the phosphodiester bond between the first and the second nucleotide of the transcript and therefore removes the whole NAD structure from the 5' end of RNA.

1.3.3. ApaH-like Phosphatases

ApaH-like phosphatases are predominantly found in prokaryotes, protists, and fungi, but are generally absent in higher eukaryotes. Bis(5'-nucleosyl)-tetraphosphatase (ApaH) was first discovered in bacteria, and it primarily hydrolyzes Ap_4A into two adenosine diphosphate (ADP) molecules. By regulating the level of Ap_4A in cells, ApaH plays a crucial role in stress response (Luciano, Levenson-Palmer and Belasco, 2019). In addition, this enzyme was described as RNA decapping enzyme cleaving bacterial Np_nN-RNAs (Hudeček *et al.*, 2020). Within eukaryotes, the ApaH-like phosphatase has mRNA decapping activity in trypanosomes, compensating for the absence of the DCP2 enzyme (Kramer, 2017). This represents the only example in eukaryotes where mRNA decapping is performed by an enzyme outside the NudiX or DXO families.

2. Aims of the Thesis

- Expression of mammalian NUDT12 enzyme in *E. coli*, followed by purification using immobilized metal affinity chromatography and size exclusion chromatography.
- Synthesis of 6-mer RNAs capped with various 5' caps by in vitro transcription, followed by purification using high-performance liquid chromatography.
- Substrate specificity analysis of mammalian NudiX enzymes using standard analytical methods (polyacrylamide gel electrophoresis and high-performance liquid chromatography).
- Development of general high-throughput method for direct comparison of NudiX activity on RNA and small molecule substrates employing the malachite green assay.

3. Material and Methods

3.1. Material

All chemicals were purchased from Merck, Sigma-Aldrich, or NEB if not described otherwise.

3.1.1. Cell Lines

E. coli BL21 transformed by pET28a plasmid for MmNUDT12, produced and described by Mititelu (2024)

3.1.2. Buffers

Annealing buffer (100 mM Tris-HCl pH 7.8, 500 mM NaCl, 10 mM EDTA)
Lysis buffer (150 mM NaCl, 50 mM sodium phosphate buffer pH 8, 10% glycerol)
Elution buffer (200 mM NaCl, 50 mM sodium phosphate buffer pH 8, 500 mM imidazole, 10% glycerol)
SEC buffer (150 mM NaCl, 50 mM Tris-HCl pH 8, 5 mM DTT)
HPLC buffer A (10 mM TEAA)
HPLC buffer B (10 mM TEAA, 90% acetonitrile)
RNA buffer A (30 mM TEAA)
RNA buffer B (30 mM TEAA, 25% acetonitrile)
NudC reaction buffer (10 mM Tris-HCl pH 7.5, 100 mM KCl, 2 mM $MgCl_2$, 2 mM DTT)
NudiX reaction buffer (100 mM Tris acetate pH 7.5, 40 mM NaCl, 10 mM megnesium acetate, 1 mM DTT)

3.1.3. Oligonucleotides

IVT 35-mer (non-template strand), Generi Biotech:
CAGTAATACGACTCACTATT**A**GGGAAGCGGGCATGCGGCCAGCCATAGCCGATCA
IVT 35-mer (template strand), Generi Biotech:
GTCATTATGCTGAGTGATAA**T**CCCTTCGCCCGTACGCCGGTCGGTATCGGCTAGT
IVT 6-mer coding (non-template strand), Generi Biotech:
CAGTAATACGACTCACTATT**A**GGGCT
IVT 6-mer coding (template strand), Generi Biotech:
GTCATTATGCTGAGTGATAA**T**CCCGA

3.1.4. Commercial Kits

Malachite Green Phosphate Assay Kit, Sigma-Aldrich (#MAK307)
Zymo RNA Clean & Concentrator Kit, Zymo Research (#R1016)
DC™ Protein Assay Kit II, Bio-Rad (#5000112)
Qubit™ RNA High Sensitivity Kit, Invitrogen (#Q32852)

3.1.5. Enzymes

T7 RNA polymerase, New England Biolabs (NEB) (#M0251)
DNAse I, NEB (#M0303)
Recombinant Shrimp Alkaline Phosphatase (rSAP), NEB (#M0371)
Pyrophosphatase, Roche (#10108987001)
HsNUDT1, HsNUDT5, HsNUDT14, HsNUDT15, HsNUDT22, Pål Stenmark group, Stockholm University
HsNUDT2, produced by (Potužník *et al.*, 2023)
MmNUDT12, produced in this study

3.1.6. RNA Caps

Ap_2A, SigutLabs
Ap_3A, SigutLabs
Ap_4A, SigutLabs
Ap_5A, Jena Bioscience (#NU-508)
Ap_2G, synthesized by Paul E. Reyes-Gutierrez (IOCB Prague)
Ap_3G, Jena Bioscience (#NU-941)
Ap_4G, Jena Bioscience (#NU-503)
Ap_5G, Jena Bioscience (#NU-504)
m^7Gp_3A, Jena Bioscience (#NU-535)
NAD, Sigma-Adrich
NADH, Sigma-Aldrich
FAD, Sigma-Aldrich
ADPR, Sigma-Aldrich

3.2. Methods

3.2.1. MmNUDT12 Expression and Purification

Gene cloning and bacterial transformation were performed by Mititelu (2024). The *Mus musculus* (Mm) NUDT12 coding sequence was inserted into a pET28a expression vector under the control of lac operon, allowing isopropyl-β-D-thiogalactopyranoside (IPTG) induction. *E. coli* BL21 (DE3) cells transformed with the expression plasmid pET28a carrying the MmNUDT12 coding sequence were cultured in 1L of Luria-Bertani medium (LB medium) containing 50 µg/mL kanamycin at 37 °C. Protein expression was induced by the addition of 0.5 mM IPTG when the culture reached an optical density at 600 nm (OD_{600}) of 0.5. Following induction, the culture was then incubated for an additional 20 hours at 20 °C. Cells were harvested by centrifugation at 6000×g for 15 minutes at 4 °C, washed with phosphate-buffered saline (PBS) and stored at -80 °C. Cell pellets were resuspended in 50 mL of Lysis buffer (composition described in Materials) containing SIGMAFAST™ Protease Inhibitor (Sigma Aldrich). Lysis was initiated by incubation with lysozyme at a final concentration of 1 mg/mL for 1 hour at 4 °C, followed by sonication in 5 cycles of 5 seconds ON and 10 seconds OFF using probe sonicator. The lysate was centrifuged at 20000×g for 45 minutes at 4 °C.

The recombinant protein construct included an N-terminal His-tag, allowing purification by immobilized metal ion affinity chromatography (IMAC) based on the affinity of histidine residues for Ni^{2+} immobilized on the column. IMAC was followed by size exclusion chromatography (SEC). Both purification steps were performed on an ÄKTA Pure system (GE Healthcare). For IMAC, the lysate was loaded on a HisTrap™ FF Crude column (Cytiva) pre-equilibrated with 4% Elution buffer (composition in Materials). Elution was performed using a linear gradient from 8% to 100% Elution buffer at a flow rate of 1 mL/min. Eluted fractions containing MmNUDT12 were further purified by SEC using a HiLoad 16/600 Superdex 75 pg column (Cytiva), equilibrated and eluted with 100% SEC buffer at a flow rate of 1 mL/min. Fractions containing MmNUDT12 were concentrated using Amicon Ultra filters with a 30 kDa molecular weight cut-off (Merck). The presence of MmNUDT12 in collected fractions was confirmed by 8% sodium dodecyl sulfate polyacrylamide gel electrophoresis (SDS-PAGE) after both IMAC and SEC. The concentration of purified MmNUDT12 protein

was determined using DC™ Protein Assay Kit II, with bovine serum albumin as a standard, and it was aliquoted and stored in SEC buffer supplemented with 10% glycerol at –80 °C.

3.2.2. Capped RNA Production

3.2.2.1. Annealing of the DNA template

Both the 6-mer and 35-mer DNA templates for IVT were prepared by annealing two complementary oligonucleotides (sequences in Materials) at 90 °C, followed by slow cooling to 20 °C. Annealing was performed in Annealing buffer (composition in Materials).

3.2.2.2. In Vitro Transcription of Radioactively Labelled Capped 35-mer RNA

In vitro transcription (IVT) was performed using T7 RNA polymerase and the annealed 35-mer DNA template containing the A φ 2.5 promoter. The 50 µL IVT reaction mixture included: 80 ng/µL DNA template, 1× RNA polymerase buffer (NEB), 5% DMSO, 4.8 mM $MgCl_2$, 0.12% Triton X-100, 12 mM DTT, 1 mM each of ATP, CTP, and UTP, 0.8 mM GTP, 0.4 µL [α-^{32}P]GTP (9.25 MBq/250 µCi in 25 µL, HARTMANN ANALYTIC), 1.6 mM cap (8 mM NAD), and 3.125 U/µL T7 RNA polymerase. The reaction was incubated at 37 °C for 2 hours. After IVT, samples were treated with DNase I at 37 °C for 1 hour, followed by enzyme inactivation at 75 °C for 10 minutes. RNA was then purified using the Zymo RNA Clean & Concentrator Kit, and concentration was determined with the Qubit RNA High Sensitivity Kit according to manufacturer's protocol.

3.2.2.3. In Vitro Transcription of Capped 6-mer RNA

IVT was performed using T7 RNA polymerase and the annealed 6-mer DNA template (sequence in Materials) containing the A φ 2.5 promoter. The 100 µL IVT reaction mixture included: 40 ng/µL of the DNA template, 1× RNA polymerase buffer (NEB), 5% DMSO, 12 mM $MgCl_2$, 0.12% triton-X 100, 50 mM DTT, 2 mM CTP, 2 mM UTP, 6 mM GTP, 2 mM cap and 0,0004 U/µL of pyrophosphatase and 5 U/µL of T7 RNA polymerase. The reaction was incubated at 37 °C for 6 hours.

3.2.2.4. Purification of Capped 6-mer RNA Using HPLC

In vitro transcribed 6-mer RNAs were first extracted using Roti®-Aqua-Phenol (Carl Roth) to denature and precipitate proteins and then using chloroform to further remove residual

protein contaminants and organic impurities. The aqueous phase containing RNA was then precipitated by ethanol in presence of 0.3 M sodium acetate (pH 5.2). The resulting RNA pellets were resuspended in DNAse- and RNase-free water and further purified on HPLC (Acquity^{TM} H-class, Waters) using XBridge^{TM} Premier Oligo C18 column (4.6 × 50 mm, 2.5 µm, Waters). RNA purification was performed at a flow rate of 1 mL/min using two buffers – RNA buffer A and RNA buffer B (composition in Materials) – and absorbance was monitored at 254 nm. A total of 13 capped RNAs were purified. Ap_2A-RNA, Ap_3A-RNA, Ap_4A-RNA and Ap_5A-RNA were purified using a 15-minute gradient: 1 minute – 94 % of A, 5 minutes – linear decrease to 60 % of A, 2 minutes – 100 % of B, 7 minutes – equilibration at 94 % of A. FAD-RNA was purified using a 15-minute gradient: 1 minute – 94 % A, 5 minutes – linear decrease to 50 % of A, 2 minutes – 100 % of B, 7 minutes – equilibration at 94 % of A. ppp-RNA, Gp_3A-RNA, Gp_4A-RNA, Gp_5A-RNA, NAD-RNA, NADH-RNA, and ADPR-RNA were purified using a 20-minute gradient: 1 minute – 94 % A, 1 minute – linear decrease to 90 % of A, 4 minutes – 90 % of A, 4 minutes – 85 % of A, 2 minutes – 100 % of B, 8 minutes – equilibration at 94 % of A.

During HPLC separation, peaks containing desired capped RNA were collected and lyophilized using a FreeZone 2.5 Freeze Dryer (Labconco) and resuspended in DNase- and RNase-free H_2O. RNA concentration was measured with a NanoDrop^{TM} One^{C} spectrophotometer (Thermo Fisher). RNA purity was verified by HPLC using the same gradients as for purification. The molecular masses of capped RNAs and potential impurities were further confirmed using LC-MS analysis.

3.2.2.5. LC-MS Analysis of HPLC-purified Capped 6-mer RNA

LC-MS spectra were measured by Dr. Anton Škríba on Acquity^{TM} H-class HPLC coupled to Xevo G2-XS QTof (Waters).

3.2.3. Analysis of NudiX Enzyme Activity toward Various Substrates

HsNUDT2 was cloned and purified by Potužník *et al.* (2023). All other NudiX enzymes, except of MmNUDT12, were provided through a collaboration with the Pål Stenmark group at Stockholm University.

3.2.3.1. Analysis of NudiX Enzyme Activity toward Small Molecules Using HPLC

To test the hydrolytic activity of HsNUDT2 and MmNUDT12 against various small substrates, 50 µL reactions were prepared containing 80 nM HsNUDT2 or 1 µM MmNUDT12, 200 µM substrate, and 5 µL of 10× NudC reaction buffer (composition in Materials). Reactions were incubated at 37 °C for 1 hour. Enzyme inactivation was performed by heating the mixture at 75 °C for 10 minutes. Following inactivation, the samples were filtered using Microcon® Centrifugal Filter columns with 10 kDa cut-off (Sigma-Aldrich). Hydrolytic activity was analyzed by HPLC (Acquity™ H-class, Waters) equipped with a Kinetex C18 column (4.6 × 150 mm, 5 µm, Phenomenex). Separation was performed at a flow rate of 1 mL/min and absorbance was monitored at 259 nm. Two buffers were used for the analysis – HPLC buffer A and HPLC buffer B (composition in materials) – with a 25-minute gradient: 2 minutes – 100 % A, 2 minutes – linear decrease to 95 % of A, 5 minutes – linear decrease to 70 % of A, 3 minutes – 70 % of A, 1 minute – linear increase to 100 % of A, 12 minutes – equilibration at 100 % of A. Substrate cleavage was quantified by calculating the ratio of the area under the curve (AUC) of peaks corresponding to substrates in the reaction mixture to the AUC of peaks corresponding to substrates in the negative control (reaction without enzyme).

3.2.3.2. Analysis of NudiX Enzyme Activity toward Capped RNA Using PAGE

To test the hydrolytic activity of HsNUDT2 and MmNUDT12 against capped RNAs, 10 µL reactions were prepared containing 80 nM HsNUDT2 or 1 µM MmNUDT12, 100 ng of in vitro transcribed RNA, and 1 µL of 10× NudC reaction buffer. Reactions were incubated at 37 °C for 1 hour. Samples were mixed with 2× RNA loading dye, denatured at 75 °C for 10 minutes and separated using 12.5% PAGE or, when required, 12.5% boronate-PAGE to improve the resolution between capped and uncapped RNA. Boronate-PAGE enables better separation of RNAs bearing caps with vicinal diols, such as NAD, and Np_nNs, while caps lacking vicinal diols, such as CoA and FAD, are not affected. The 12.5% PAGE was prepared using 21 mL of 25% Rotiphorese® (Carl Roth), 21 mL of 2× TBE, 340 µL of APS and 16.8 µL of TEMED. For boronate-PAGE, 150 mg of boronic acid was additionally included in the gel mixture. The PAGE was performed at 600V for 4 hours. Radiolabeled RNA was visualized using a Typhoon FLA 9500 scanner. The RNA cap cleavage was quantified by calculating the ratio of band intensities corresponding to capped RNA to the band intensities of the negative control (reaction without enzyme). Band intensities were quantified using ImageJ software.

3.2.3.3. Analysis of NudiX Enzyme Activity toward Various Substrates Using Malachite Green Phosphate Assay Kit

NUDIX enzymes – HsNUDT1, HsNUDT2, HsNUDT5, MmNUDT12, HsNUDT14, HsNUDT15, and HsNUDT22 were screened toward 12 small molecules (Ap_2A, Ap_3A, Ap_4A, Ap_5A, Gp_3A, Gp_4A, Gp_5A, m^7Gp_3A, NAD, NADH, FAD, and ADPR) and ten capped RNAs (Ap_2A-RNA, Ap_3A-RNA, Ap_4A-RNA, Ap_5A-RNA, Gp_3A-RNA, Gp_4A-RNA, Gp_5A-RNA, m^7Gp_3A-RNA, NAD-RNA, and FAD-RNA) using Malachite Green Phosphate Assay Kit. Additionally, HsNUDT1 and HsNUDT15 were tested also toward dGTP, ATP and ppp-RNA. 20 µL of reaction mixture contained: 100 nM or 1 µM NudiX, 5 µM substrate, 0,01 U/µL of rSAP or 0,002 U/µL of pyrophosphatase and 2 µL of 10× NudiX reaction buffer (composition in Materials). Reactions were incubated at 37 °C for 30 minutes in a 384-well plate.

The enzymatic reaction was stopped by the addition of 5 µL Malachite Green Working Reagent, prepared according to the manufacturer's instructions. After a 30-minute incubation, absorbance was measured at 620 nm using a TECAN SPARK® plate reader. A standard curve was generated according to the manufacturer's protocol. The statistical differences between mean values were calculated using multiple unpaired t-test followed by Holm-Šidák correction with significance level α of 0.05. All graphs and statistical analyses were generated in GraphPad Prism 10.4.2.

4. Results

4.1. MmNUDT12 Expression and Purification

As part of the research team that discovered a novel RNA cap structure, Ap_2A-RNA, I participated in studies investigating its processing. Based on the structural similarity between Ap_2A and previously characterized NAD cap, we hypothesized that NUDT12, known as a deNADing enzyme, might also be capable of removing the Ap_2A cap from RNA. For this reason, NUDT12 was selected as one of the candidates for substrate specificity testing.

In order to enable characterization of NUDT12, the first objective of my master's thesis was to express and purify recombinant MmNUDT12 from *E. coli* BL21 cells. The expression was performed in 1L of *E. coli* culture. The expressed protein containing an N-terminal His-Tag, was purified using IMAC, based on the affinity of histidine residues for Ni^{2+} immobilized on the column. Followingly, SEC was used to remove non-specifically bound proteins that also interacted with the Ni^{2+} but differed in size from MmNUDT12. Protein fractions were analyzed by SDS-PAGE after both IMAC and SEC purification steps.

During IMAC, MmNUDT12 was eluted in response to the increasing concentration of imidazole in elution buffer (Figure 7A). The small size of the elution peak (indicated by the arrow in Figure 7A) suggests that only a limited amount of protein was retained on the column and subsequently eluted. In SDS-PAGE analysis, the eluted protein was detected as a band migrating between the 40 kDa and 70 kDa markers (Figure 7B), consistent with the calculated molecular weight of MmNUDT12 (51.5 kDa). MmNUDT12 was present in fractions 2-6. These fractions were pooled and further purified by SEC.

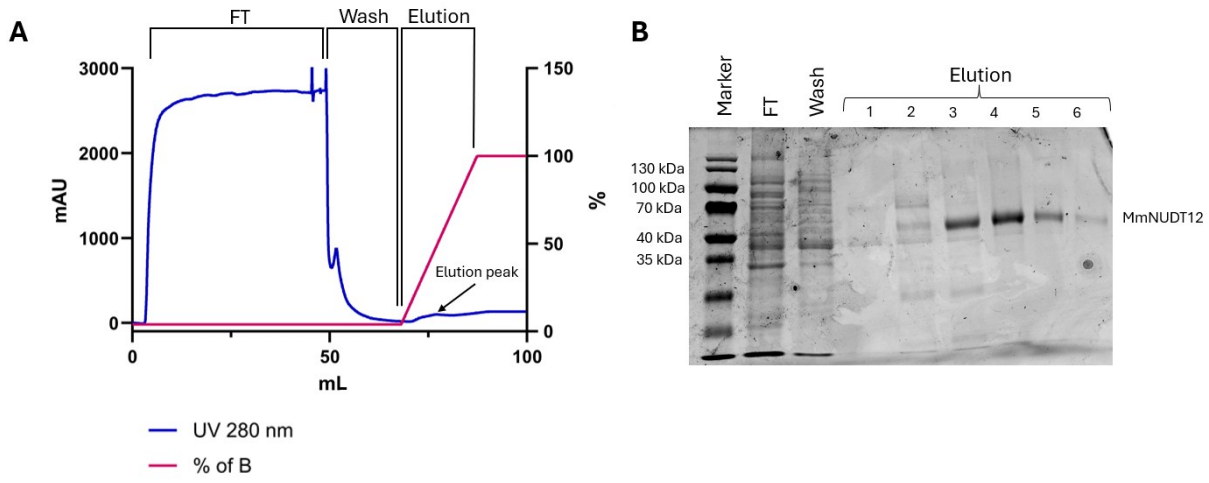

***Figure 7**: **(A)** Chromatogram from ÄKTA Pure instrument showing the IMAC purification. The X-axis represents volume (mL), the left Y-axis shows absorbance of 280 nm in milli-arbitrary units (mAU), and the right Y-axis indicates the percentage (%) of elution buffer (B). The blue line corresponds to the absorbance at 280 nm (left Y-axis). The magenta line represents the gradient of B (right Y-axis). The positions of the flow-through (FT) and elution fractions (Elution) collected for SDS-PAGE analysis are indicated above the chromatogram. **(B)** 8% SDS-PAGE analysis of MmNUDT12 after purification by IMAC. The gel includes molecular weight marker (PageRuler Prestained Protein Ladder, 10 – 180 kDa, Thermo Fisher), flow-through (FT), wash fraction (Wash) and 6 elution fractions (Elution).*

The chromatogram from SEC contained two small elution peaks (Figure 8A). Both were analyzed by SDS-PAGE, which confirmed the presence of MmNUDT12 in both peaks, as indicated by bands corresponding to its expected molecular weight of 51.5 kDa (Figure 8B).

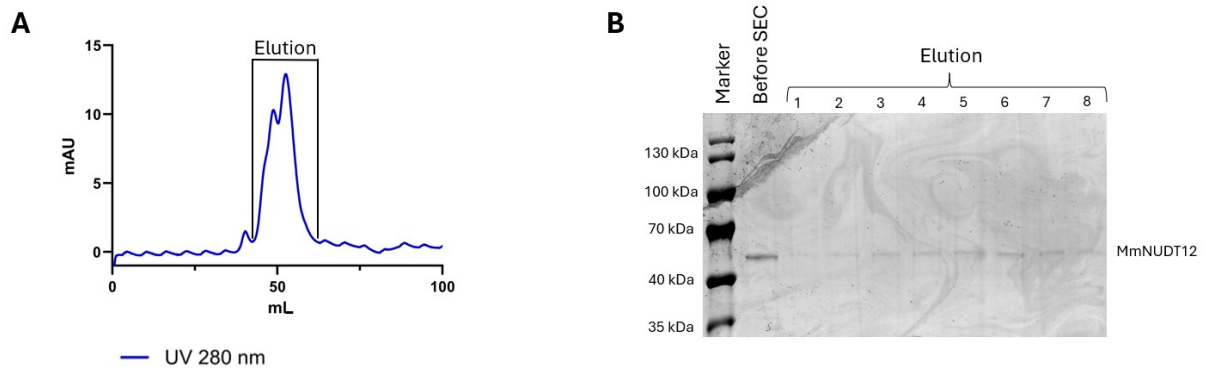

***Figure 8**: **(A)** Chromatogram from ÄKTA Pure instrument showing the SEC purification. The X-axis represents volume (mL) and the Y-axis shows absorbance in mAU. The blue line corresponds to the absorbance at 280 nm. Elution fractions (Elution) collected for SDS-PAGE analysis are indicated above the chromatogram. **(B)** 8% SDS-PAGE analysis of MmNUDT12 after purification by SEC. Gel includes molecular weight marker (PageRuler Prestained Protein Ladder, 10 – 180 kDa, Thermo Fisher), sample before SEC purification (Before SEC) and 8 elution fractions collected during SEC (Elution).*

The final yield of purified MmNUDT12 from 1 L of bacterial culture was 0.4 mg. Although the expression was successful, the yield was relatively low, which may be caused by losses during purification.

4.2. Capped RNA Production

Synthesis of RNA substrates was a necessary step to investigate the decapping activity of NudiX enzymes on various capped RNAs. Thirteen 6-mer RNAs were prepared, each carrying a different 5' modification – twelve capped RNAs and 5' triphosphate RNA (ppp-RNA). The RNAs were synthesized by IVT, followed by phenol–chloroform extraction to remove proteins and other contaminants. The IVT reactions were then purified by HPLC to separate the capped RNA from incomplete products and free caps. After purification, the RNAs were lyophilized, resuspended in RNase- and DNase-free H_2O, and their concentrations were measured using a NanoDrop™ OneC spectrophotometer.

To illustrate how the RNA sample looked before HPLC purification, one representative chromatogram is shown, including the collection of the peak corresponding to the capped-RNA – in this case Gp_3A-RNA – with the correct molecular mass (Figure 9; Table 2).

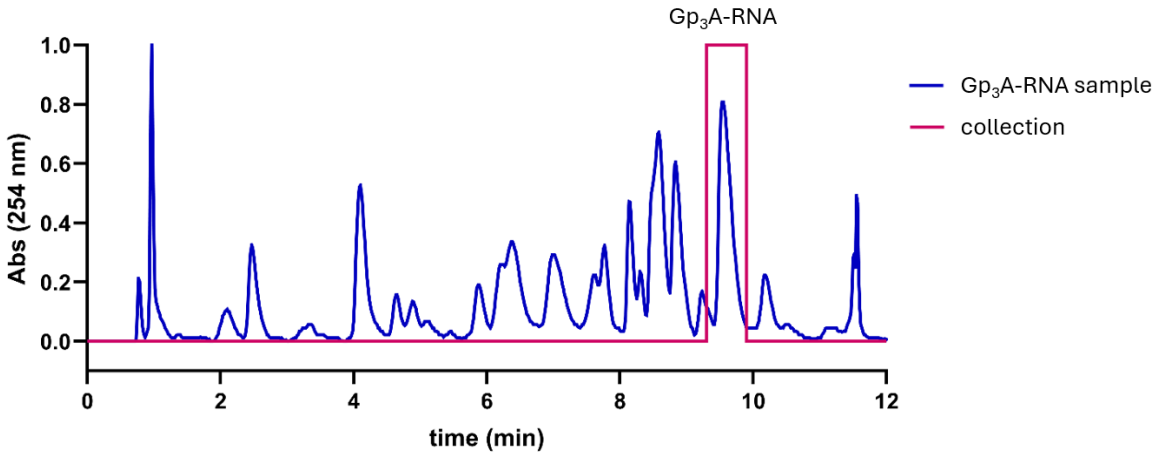

***Figure 9**: Representative chromatogram showing the Gp_3A-RNA sample after IVT and phenol-chloroform extraction. The blue line represents absorbance (mAU) of the RNA sample, and the magenta line indicates the collected peak corresponding to the capped RNA with the correct molecular mass.*

Of the twelve capped RNAs, ten were successfully purified to a final purity equal to or higher than 80% (Figure 10; Table 2). These included Ap_2A-RNA, Ap_3A-RNA, Ap_4A-RNA, Ap_5A-RNA, Gp_3A-RNA, Gp_4A-RNA, Gp_5A-RNA, m^7Gp_3A-RNA, NAD-RNA,

and FAD-RNA. In contrast, two capped RNAs – NADH-RNA and ADPR-RNA – were not successfully purified. NADH-RNA is highly unstable and oxidizes very easily to NAD-RNA during manipulation. ADPR-RNA could not be separated from p-RNA under the conditions used. The ppp-RNA was also purified successfully.

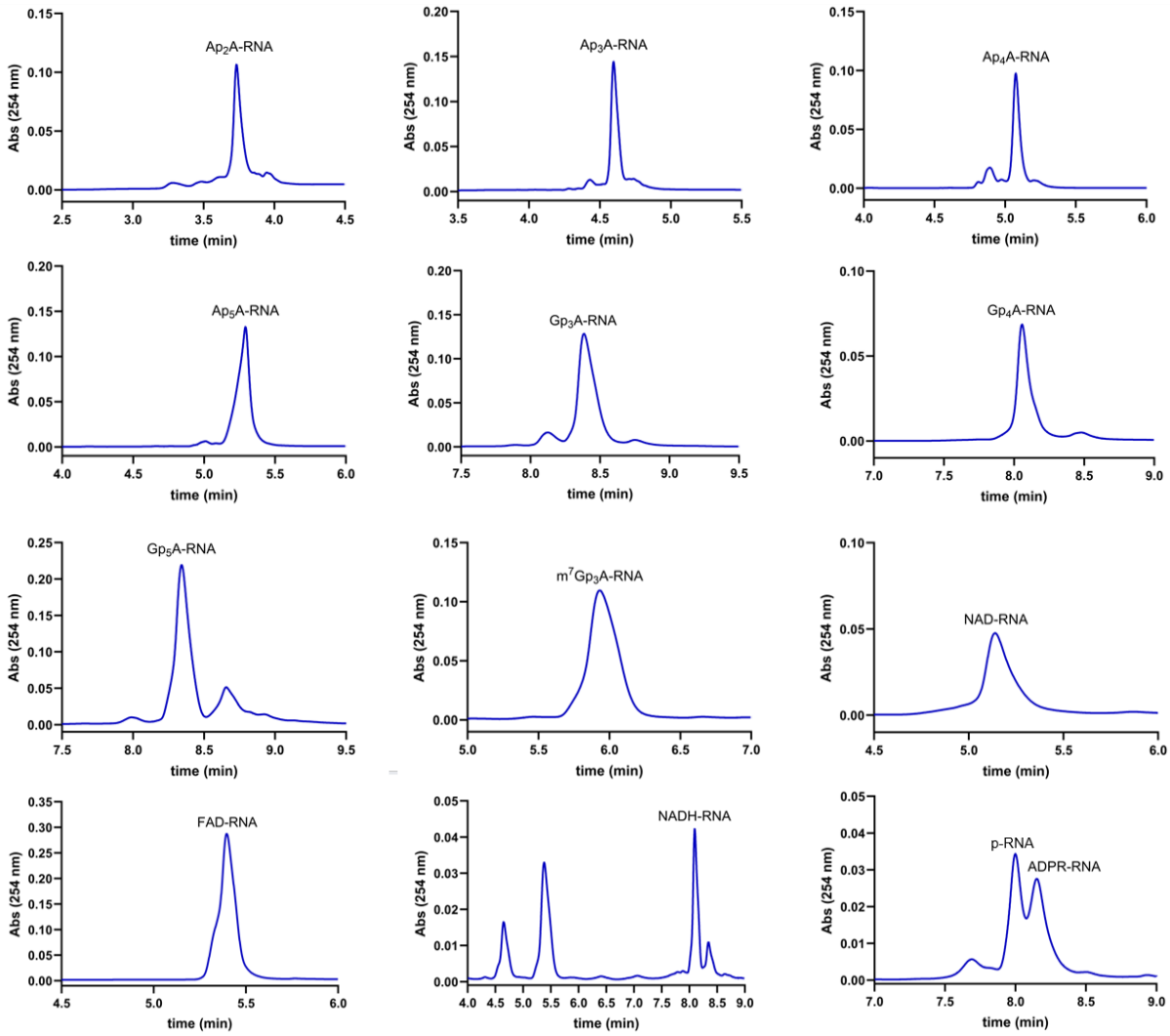

***Figure 10**: Chromatograms of purified capped 6-mer RNAs. Chromatograms show different RNA samples, demonstrating successful purification (purity ≥ 80%) for ten capped RNAs and unsuccessful purification (purity < 80%) for two capped RNAs (NADH- and ADPR-RNA). Peaks corresponding to capped RNAs with the correct molecular mass are indicated.*

The purity of RNA was calculated from the chromatograms as the AUC of the product divided by the total AUC of all detected peaks. Analysis of isolated RNA was performed by Dr. Anton Škríba employing LC-MS. Table 2 summarizes the sequence, calculated molecular mass, experimentally determined molecular mass, and final purity of each RNA sample, confirming the successful preparation of ten RNA substrates for the subsequent enzymatic studies.

The purity of NADH-RNA and ADPR-RNA was below 80%, and therefore, these two capped RNAs were not included in the table, nor were they included in further enzymatic assays. Additionally, the experimentally determined molecular mass of Gp_4A-RNA was found to be 16 Da higher than the calculated value. This discrepancy is further discussed in the Discussion section.

***Table 2**: Summary of purified 6-mer RNAs. For each RNA sample, purity, calculated molecular mass and experimentally determined molecular mass (measured by LC-MS) are shown. Purity was determined from the HPLC chromatograms as the ratio of the AUC of the product to the total AUC of all detected peaks.*

Sample	Purity (%)	Molecular mass of $[M-2H]^{2-}$ (Da)	
		Calculated	Found
Ap_2A-RNA	88	1160.1550	1160.1460
Ap_3A-RNA	92	1200.1381	1200.1271
Ap_4A-RNA	80	1240.1213	1240.1075
Ap_5A-RNA	100	1280.1045	1280.0912
Gp_3A-RNA	91	1208.1356	1208.1228
Gp_4A-RNA	96	1248.1188	1256.1003
Gp_5A-RNA	82	1288.1019	1288.0865
m^7Gp_3A-RNA	100	1215.1434	1215.1271
NAD-RNA	100	1153.6517	1153.6423
FAD-RNA	100	1214.6757	1214.6626

4.3. Activity of NudiX Enzymes toward Various Substrates

Some NudiX hydrolases have been identified as RNA decapping enzymes, capable of removing non-canonical caps such as NAD or Ap_4A from the 5′ end of RNA (Potužník *et al.*, 2023; Cahová *et al.*, 2015). However, the majority of NudiX family members have not been systematically tested for this activity. This knowledge gap provided motivation for this study, which aimed to evaluate the potential RNA decapping activity of selected NudiX enzymes and to compare their activity toward capped RNA with their activity toward corresponding small molecules.

In order to provide a reference point for further screening with a broader number of NudiX enzymes and substrates and to verify the enzymatic activity of MmNUDT12 after purification, the activities of HsNUDT2 and MmNUDT12 were evaluated on both small molecules and capped RNAs. This analysis was performed using a well-established approach routinely applied in Hana Cahová's laboratory (Mititelu *et al.*, 2023). Hydrolysis of small molecules was analyzed by HPLC, while RNA cleavage was analyzed by PAGE.

4.3.1. Activity of NudiX Enzymes toward Small Molecules Evaluated by HPLC

4.3.1.1. Activity of HsNUDT2

The hydrolytic activity of HsNUDT2 toward small molecules was assessed using 80 nM HsNUDT2 and 200 µM substrate. Each reaction was performed in triplicate to ensure reproducibility. To illustrate the reaction outcomes, two representative HPLC chromatograms are shown (Figure 11). These examples demonstrate that HsNUDT2 does not cleave Ap_3A, whereas it quantitatively cleaves Ap_4A under the same conditions.

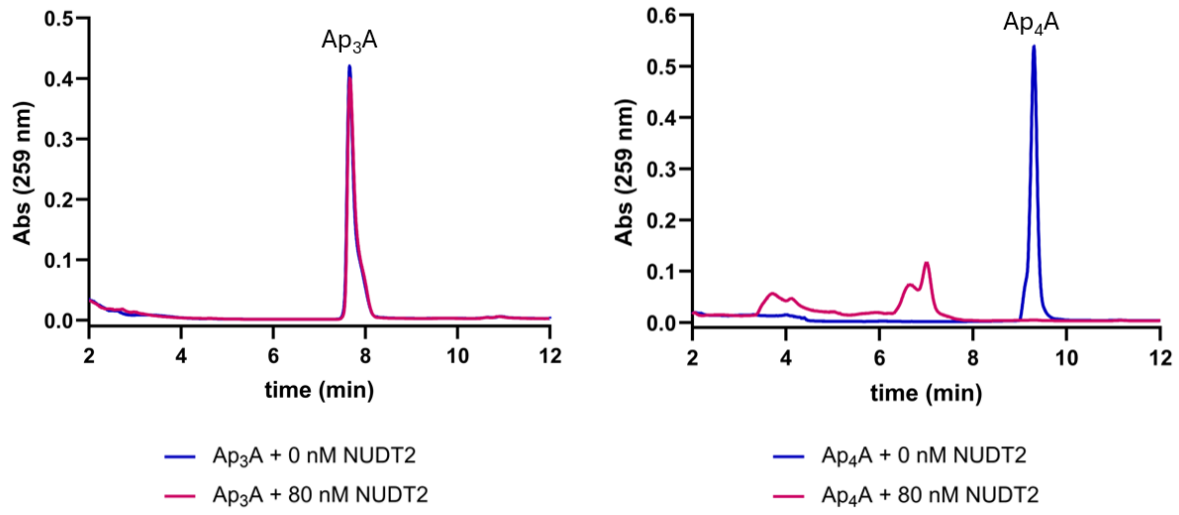

***Figure 11**: Two representative chromatograms showing HPLC analysis of HsNUDT2 activity toward two substrates – Ap_3A (left) and Ap_4A (right). In each chromatogram, the magenta line represents the reaction with HsNUDT2, and the blue line represents the negative control without enzyme. Ap_4A peak disappearance indicates substrate cleavage by HsNUDT2. The X-axis represents retention time (minutes), and the Y-axis shows absorbance (Abs) at 259 nm.*

HsNUDT2 was tested against 10 small molecules: Ap_2A, Ap_3A, Ap_4A, Ap_5A, Gp_2A, Gp_3A, Gp_4A, Gp_5A, NAD, and FAD (Figure 12). HsNUDT2 efficiently cleaved dinucleoside polyphosphates with four or five phosphate groups (Np_4Ns and Np_5Ns). Among the tested

substrates, Ap_4A was the most efficiently hydrolyzed (97.3 ± 5.3%), followed by Gp_4A, Gp_5A, and Ap_5A. In contrast, no hydrolytic activity was observed for the other six substrates. These results suggest that Ap_4A is the preferred substrate of HsNUDT2 under the tested conditions.

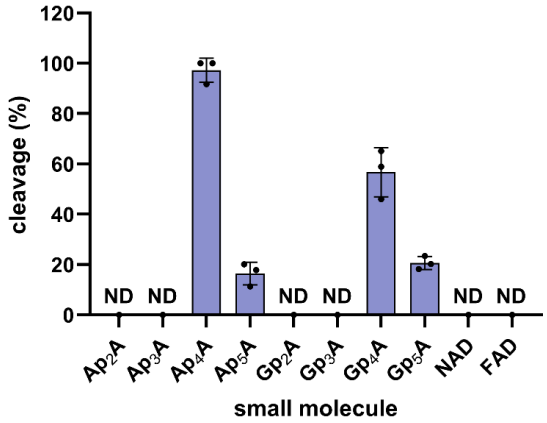

***Figure 12**: Cleavage of small molecules by HsNUDT2. The graph shows the percentage of substrate hydrolysis by 80 nM HsNUDT2 after 1-hour incubation at 37 °C with 200 µM substrate. Data are presented as mean ± standard deviation (SD) from three independent experiments. ND = not detected (cleavage less than 5% observed under the tested conditions).*

4.3.1.2. Activity of MmNUDT12

The enzymatic activity of purified MmNUDT12 was evaluated by testing the enzyme toward its previously reported substrates – Ap_2A, and NAD (Abdelraheim, Spiller and McLennan, 2003) – as well as Ap_2G, a structurally related dinucleotide not previously described as a substrate of MmNUDT12. (Figure 13). Each reaction was performed in duplicate using 1 µM MmNUDT12 and 200 µM substrate. Hydrolytic activity was observed for all three substrates. Among them, Ap_2G was the most efficiently hydrolyzed (98.3 ±0.1%), followed by Ap_2A, and NAD.

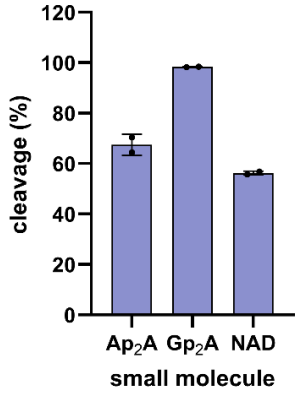

Figure 13: *Cleavage of small molecules by MmNUDT12. The graph shows the percentage of substrate hydrolysis by 1 µM MmNUDT12 after 1-hour incubation at 37 °C with 200 µM substrate. Data are presented as mean ± SD from two independent experiments.*

4.3.2. Activity of NudiX Enzymes toward Capped RNA Evaluated by PAGE

4.3.2.1. Activity of HsNUDT2

The enzymatic activity of HsNUDT2 on capped 35-mer RNAs was analyzed using 12.5% PAGE (Figure 14) or 12.5% boronate-PAGE (Figure 15), with radiolabeled RNA transcripts. In total, 10 different capped RNAs were tested: Ap_2A-RNA, Ap_3A-RNA, Ap_4A-RNA, Ap_5A-RNA, Gp_2A-RNA, Gp_3A-RNA, Gp_4A-RNA, Gp_5A-RNA, NAD-RNA, and FAD-RNA. Each reaction was performed in duplicate using 80 nM HsNUDT2 and 100 ng of in vitro transcribed RNA. A representative PAGE result is shown for each capped RNA. While most RNAs were analyzed using standard PAGE, Ap_2A-, Ap_2G-, NAD-, and FAD-capped RNAs were analyzed on 12.5% boronate-containing PAGE, which provides better resolution of capped versus uncapped RNA compared to standard PAGE. Although FAD-capped RNA was also run on boronate-PAGE, it does not enhance its separation, as FAD lacks vicinal diol structures required for interaction with boronic acid.

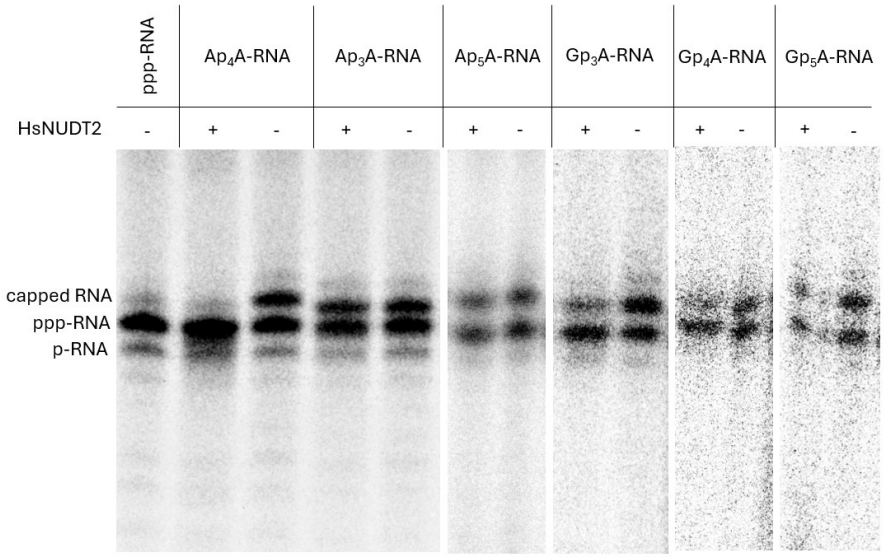

***Figure 14**: 12.5% PAGE analysis of capped RNA cleavage by HsNUDT2. Each lane contains 100 ng of in vitro transcribed RNA incubated with or without 80 nM HsNUDT2.*

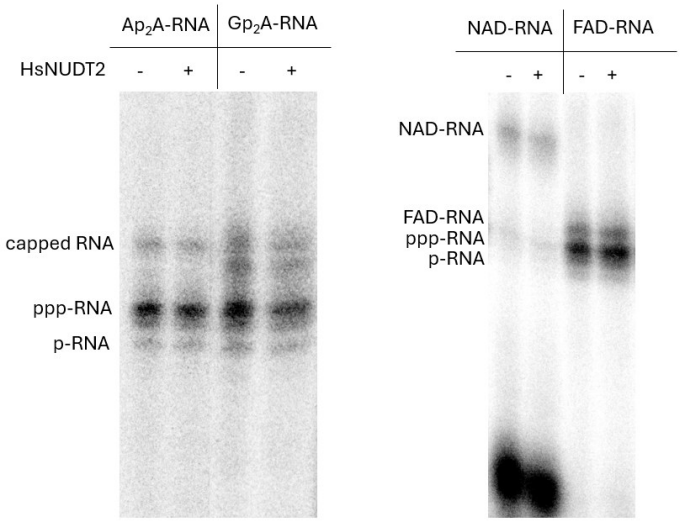

***Figure 15**: 12.5% boronate-PAGE analysis of capped RNA cleavage by HsNUDT2. Each lane contains 100 ng of in vitro transcribed RNA incubated with or without 80 nM HsNUDT2.*

In case of capped RNAs, HsNUDT2 efficiently cleaved Np_4Ns- and Np_5Ns-capped RNAs, consistent with its activity on corresponding small molecules. Unlike with small molecules, HsNUDT2 also cleaved Gp_3A-RNA (Figure 16). Among the tested substrates, Ap_4A-RNA was the most efficiently hydrolyzed (78.4 ± 2.7%), followed by Gp_4A-RNA, Gp_3A-RNA, Gp_5A-RNA, and Ap_5A-RNA. These findings suggest that Ap_4A-RNA may be the preferred substrate of HsNUDT2 under the tested conditions.

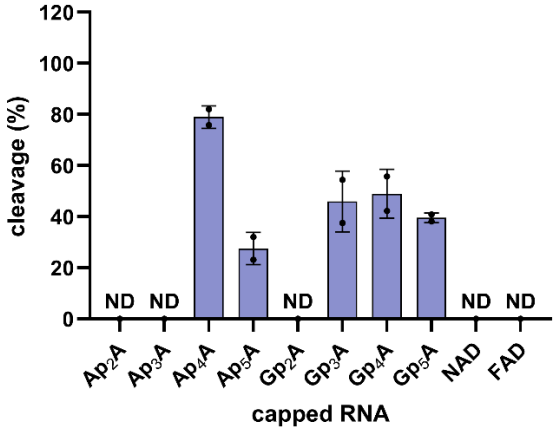

***Figure 16**: Cleavage of capped RNAs by HsNUDT2. The graph shows the percentage of substrate hydrolysis by 80 nM HsNUDT2 after 1-hour incubation at 37 °C with 100 ng of in vitro transcribed RNA. Data are presented as mean ± SD from two independent experiments. ND = not detected (cleavage less than 5% observed under the tested conditions).*

4.3.2.2. Activity of MmNUDT12

The enzymatic activity of MmNUDT12 was evaluated on three capped 35-mer RNAs, each corresponding to a tested small molecule: Ap_2A-RNA, Gp_2A-RNA, and NAD-RNA. The cleavage of tested capped RNA was analyzed using 12.5% boronate-PAGE with radiolabeled RNA transcripts (Figure 17). Each reaction was performed in duplicate using 1 µM MmNUDT12 and 100 ng of in vitro transcribed RNA.

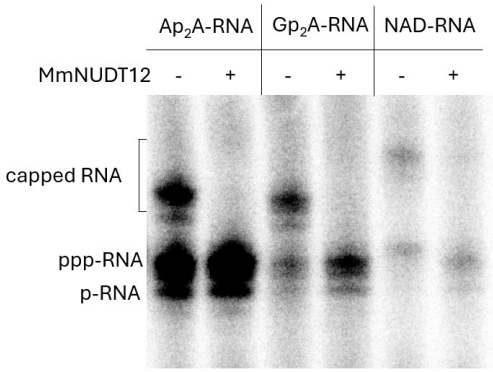

***Figure 17**: 12.5% boronate-PAGE analysis of capped RNA cleavage by MmNUDT12. Each lane contains 100 ng of in vitro transcribed RNA incubated with or without 1 µM MmNUDT12.*

The hydrolytic activity of MmNUDT12 was observed toward all three tested substrates (Figure 18). Ap_2G-RNA and Ap_2A-RNA were hydrolyzed the most efficiently (98.3 ± 0.1% and 99.6 ± 0.2%, respectively), followed by NAD-RNA.

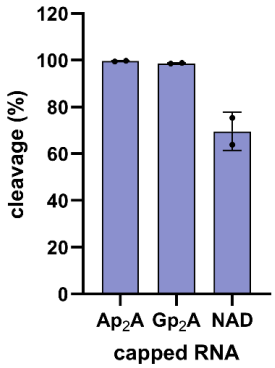

***Figure 18**: Cleavage of capped RNAs by MmNUDT12. The graph shows the percentage of substrate hydrolysis by 1 µM MmNUDT12 after 1-hour incubation at 37 °C with 100 ng of in vitro transcribed RNA. Data are presented as mean ± SD from two independent experiments.*

4.3.3. Activity of NudiX Enzymes toward Various Substrates Evaluated by MGA

A direct comparison of cleavage efficiency between small molecules and RNA substrates using HPLC and PAGE was problematic because of the different method sensitivity and substrate concentration requirements for these two methods. HPLC requires significantly higher substrate concentrations than PAGE, making it technically challenging to analyze small molecules and capped RNAs at equivalent concentrations. To address this limitation, the malachite green assay (MGA) was employed. As a high-throughput method, MGA allows for direct comparison of small-molecule and RNA cleavage by using an equivalent substrate concentration and detection approach. The MGA has previously been applied to study the activity of NudiX enzymes toward small molecules *(*Carreras-Puigvert *et al., 2017)*. The aim of this part of work was to extend this methodology to RNA substrates.

Malachite green assay is a colorimetric method widely used for the detection and quantification of free inorganic phosphate (P_i) released during enzymatic reactions. In this assay, molybdate reacts with inorganic phosphate to form a phosphomolybdate complex, which is subsequently detected through a colorimetric reaction with malachite green dye, producing a measurable green color with an absorbance maximum at 620 nm (Figure 19). The intensity of this color

is directly proportional to the concentration of P_i in the sample (Baykov, Evtushenko and Avaeva, 1988). Since most NudiX-catalyzed reactions result in the release of pyrophosphate (PP_i) or nucleoside polyphosphates, which do not directly react in the malachite green assay, additional enzymatic reaction was required to generate measurable P_i. For this purpose, reactions were supplemented with either rSAP or PPH, depending on the nature of the cleavage product, to convert PP_i or other phosphate-containing molecules into P_i. This allowed for accurate quantification of NudiX cleavage efficiency by the MGA.

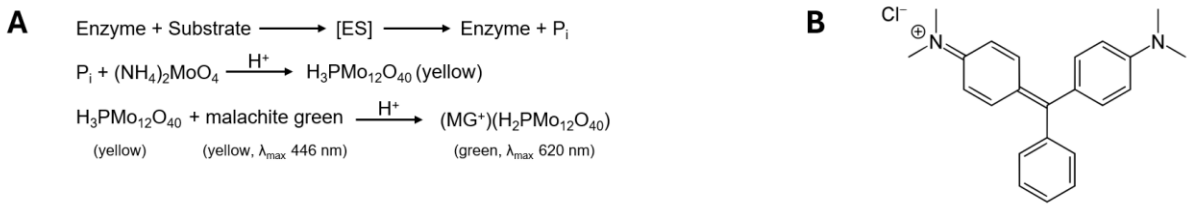

Figure 19: ***(A)*** *Schematic representation of the malachite green assay used for inorganic phosphate detection.* ***(B)*** *Chemical structure of malachite green.*

First, a standard calibration curve to quantify the concentration of P_i was generated using serial dilutions of phosphate standard provided in the Malachite Green Phosphate Assay Kit under the same conditions used for the enzymatic reactions with NudiX enzymes (Figure 20). This calibration curve was then used to convert measured absorbance values to phosphate concentrations, enabling comparison across samples.

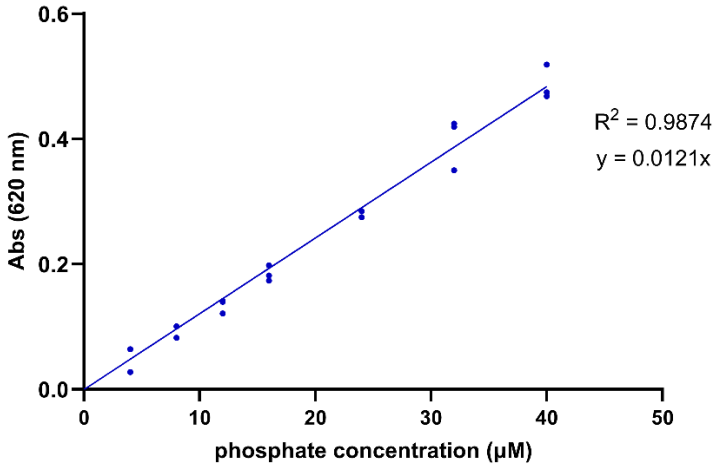

Figure 20*: Calibration curve of inorganic phosphate (P_i) generated from serial dilutions of phosphate standard. Absorbance at 620 nm is plotted against phosphate concentration. The coefficient of determination (R^2) indicates the linearity and reliability of the standard curve fit.*

The resulting linear regression equation used for the calculation of P_i concentration in the enzymatic reactions was:

$$[\mathbf{P_i}] = \frac{\mathbf{Abs\ (620\ nm)}}{\mathbf{0.0121}}$$

where *Abs (620 nm)* is the absorbance at 620 nm and *[P_i]* is the concentration of released inorganic phosphate (µM). This equation was applied for the determination of cap cleavage in each enzymatic reaction. Since the substrate concentration was fixed at 5 µM, the calculated P_i concentration was normalized to the number of phosphate groups present in each cap structure.

MGA was employed for a direct comparison of small-molecule cleavage and RNA cleavage by mammalian NudiX enzymes. In total, seven NudiX enzymes – HsNUDT2, and MmNUDT12 (purified in Hana Cahová group), and HsNUDT1, HsNUDT15, HsNUDT5, HsNUDT14 and HsNUDT22 (provided by Pål Stenmark) – were tested toward twelve small molecules (Ap_2A, Ap_3A, Ap_4A, Ap_5A, Gp_3A, Gp_4A, Gp_5A, m^7Gp_3A, NAD, NADH, FAD, and ADPR) and ten capped RNAs (Ap_2A-RNA, Ap_3A-RNA, Ap_4A-RNA, Ap_5A-RNA, Gp_3A-RNA, Gp_4A-RNA, Gp_5A-RNA, m^7Gp_3A-RNA, NAD-RNA, and FAD-RNA). In addition, HsNUDT1 and HsNUDT15 were also tested toward dGTP, their known substrate, as well as ATP and ppp-RNA, since these substrates are relevant to their reported triphosphatase activity. All enzymes, except MmNUDT12, were used at a final concentration of 100 nM, MmNUDT12 was used at a final concentration of 1 µM. Enzymes were incubated with 5 µM substrate for 30 minutes at 37 °C. All measurements presented in this section were performed in triplicate.

The first enzyme tested, HsNUDT2, has previously been identified as an Ap_4A-RNA decapping enzyme, as reported in the literature (Potužník *et al.*, 2023; Table 1). This activity was also confirmed in this thesis by PAGE analysis (Figure 16). Using the MGA, HsNUDT2 was found to hydrolyze four tested small molecules – Ap_4A, Ap_5A, Gp_4A, and Gp_5A– as well as their corresponding capped RNAs – Ap_4A-RNA, Ap_5A-RNA, Gp_4A-RNA, and Gp_5A-RNA (Figure 21). These results are consistent with the HPLC analysis, which also showed hydrolysis of Ap_4A, Ap_5A, Gp_4A and Gp_5A. In the case of capped RNAs, MGA revealed cleavage only of Ap_4A-RNA, Ap_5A-RNA, Gp_4A-RNA, and Gp_5A-RNA, whereas PAGE analysis additionally showed activity toward Gp_3A-RNA, and NAD-RNA. Moreover, the MGA results

demonstrated that HsNUDT2 exhibited significantly higher activity toward Ap_4A-RNA than Ap_4A, Ap_5A-RNA than Ap_5A, and Gp_5A-RNA than Gp_5A. On the other hand, this enzyme exhibited significantly higher activity toward Gp_4A than Gp_4A-RNA.

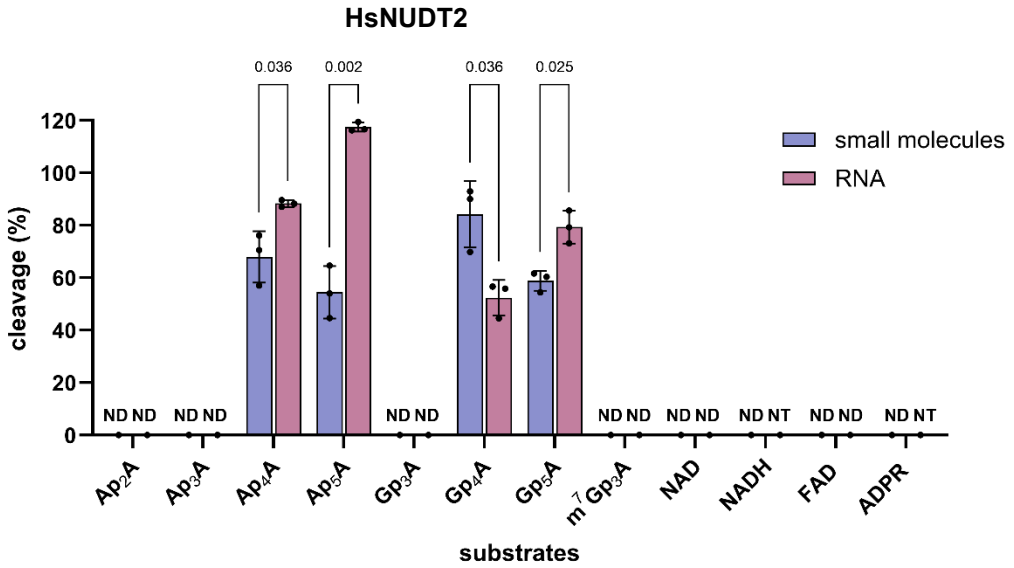

***Figure 21**: Cleavage of small molecules and capped RNAs by HsNUDT2. The graph shows the percentage of substrate hydrolysis by 100 nM HsNUDT2 after 30-minute incubation at 37 °C with 5 µM substrate measured by MGA. Data are presented as mean ± SD from three independent experiments. ND = not detected (cleavage less than 5% observed under the tested conditions), NT = not tested. Statistical differences between small molecules and RNA are expressed as adjusted P values.*

Initial testing of MmNUDT12 using MGA was performed at a final concentration of 100 nM, consistent with the conditions used for other NudiX enzymes. However, under these conditions, no cleavage activity was observed toward its expected substrate, Ap_2A. Therefore, the enzyme concentration was increased to 1 µM for further testing. At this concentration, MmNUDT12 exhibited hydrolytic activity toward ten out of twelve tested small molecules: Ap_2A, Ap_3A, Ap_4A, Ap_5A, Gp_3A, m^7Gp_3A, NAD, NADH, FAD, and ADPR. Among the ten capped RNAs, six were cleaved by MmNUDT12: Ap_2A-RNA, Ap_3A-RNA, Ap_4A-RNA, Ap_5A-RNA, Gp_4A-RNA, and NAD-RNA (Figure 22). These results are consistent with those obtained from HPLC and PAGE analyses, which previously identified Ap_2A, NAD, Ap_2A-RNA, and NAD-RNA as substrates of MmNUDT12. Notably, the only significant difference in activity between the small molecule and corresponding RNA cap, was observed for Ap_2A and Ap_2A-RNA, where the small-molecule form was hydrolyzed more efficiently.

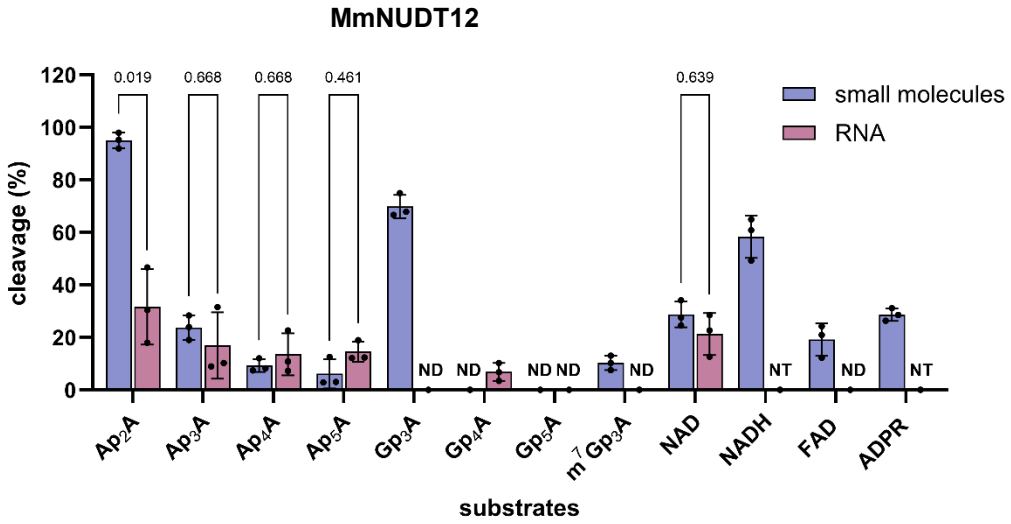

***Figure 22**: Cleavage of small molecules and capped RNAs by MmNUDT12. The graph shows the percentage of substrate hydrolysis by 1 µM MmNUDT12 after 30-minute incubation at 37 °C with 5 µM substrate measured by MGA. Data are presented as mean ± SD from three independent experiments. ND = not detected (cleavage less than 5% observed under the tested conditions), NT = not tested. Statistical differences between small molecules and RNA are expressed as adjusted P values.*

HsNUDT1 is known to cleave dNTPs and their derivatives (Carreras-Puigvert *et al*., 2017), and therefore dGTP was tested as a first substrate to test whether the enzyme is active under these conditions. dGTP was cleaved with an efficiency of 47.5 ± 6.5%, and among all tested substrates, it was the only one hydrolyzed under these conditions (Figure 23).

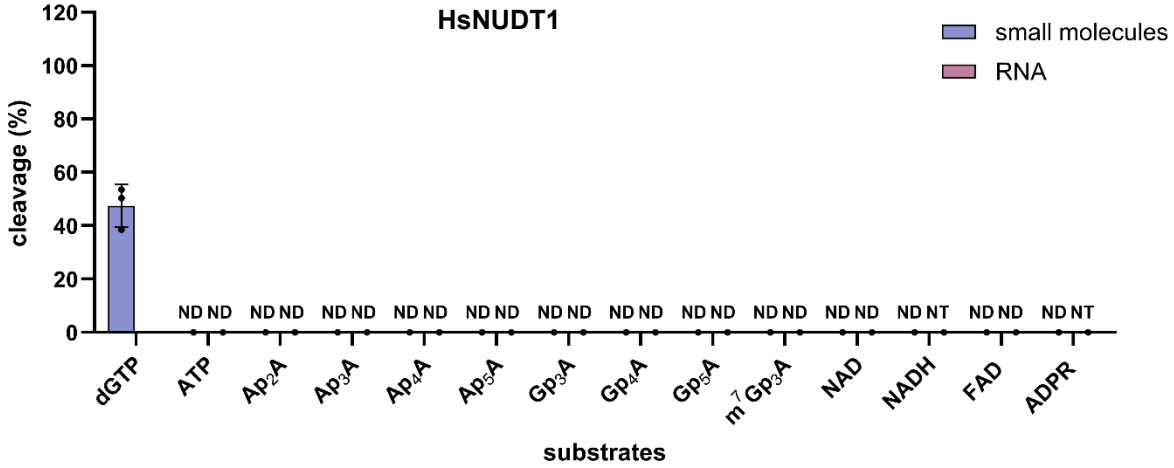

***Figure 23**: Cleavage of small molecules and capped RNAs by HsNUDT1. The graph shows the percentage of substrate hydrolysis by 100 nM HsNUDT1 after 30-minute incubation at 37 °C with 5 µM substrate measured by MGA. Data are presented as mean ± SD from three independent experiments. ND = not detected (cleavage less than 5% observed under the tested conditions), NT = not tested.*

Another enzyme known to hydrolyze dNTPs, NTPs, and their derivatives is HsNUDT15 (Carreras-Puigvert *et al*., 2017). Similar to HsNUDT1, its activity was first confirmed using dGTP as a substrate. The enzyme was then tested against a broader panel of substrates, including ATP and ppp-RNA. dGTP was cleaved with an efficiency of 49.4 ± 9.6%. In addition to dGTP, Gp_5A-RNA was also hydrolyzed, but only by 11.6 ± 1.9%. None of the other tested substrates were hydrolyzed by HsNUDT15 under the conditions used (Figure 24).

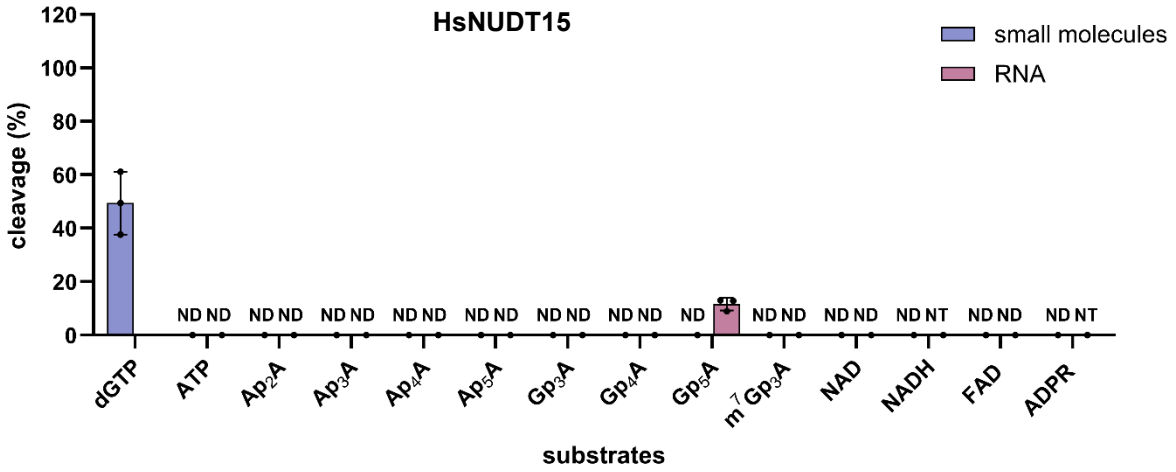

Figure 24*: Cleavage of small molecules and capped RNAs by HsNUDT15. The graph shows the percentage of substrate hydrolysis by 100 nM HsNUDT15 after 30-minute incubation at 37 °C with 5 μM substrate measured by MGA. Data are presented as mean ± SD from three independent experiments. ND = not detected (cleavage less than 5% observed under the tested conditions), NT = not tested.*

The next enzyme analyzed was HsNUDT5. According to literature, this enzyme preferentially hydrolyzes ADP-sugars and NADH (Carreras-Puigvert *et al.*, 2017). HsNUDT5 exhibited activity toward four small molecules: Ap_2A, NADH, FAD and ADPR, with ADPR being the most efficiently cleaved. HsNUDT5 did not exhibit any activity toward capped RNAs (Figure **25**).

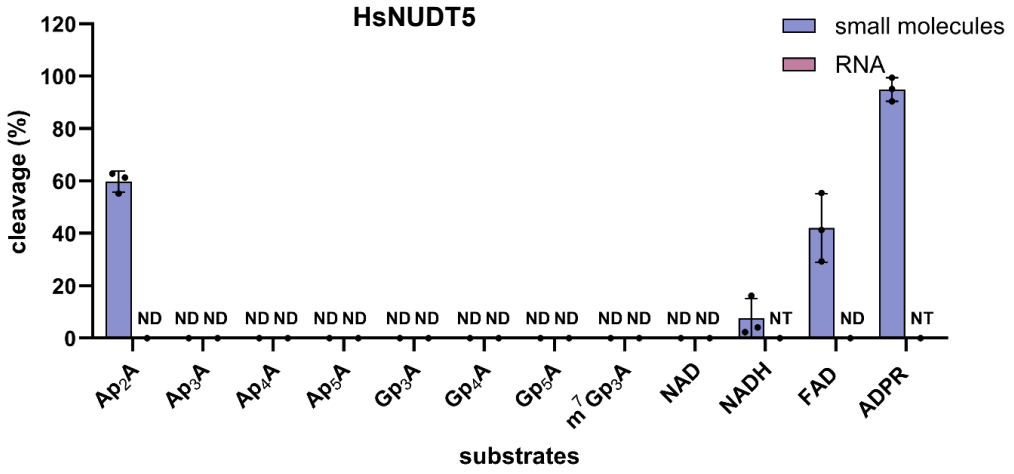

***Figure 25**: Cleavage of small molecules and capped RNAs by HsNUDT5. The graph shows the percentage of substrate hydrolysis by 100 nM HsNUDT5 after 30-minute incubation at 37 °C with 5 µM substrate measured by MGA. Data are presented as mean ± SD from three independent experiments. ND = not detected (cleavage less than 5% observed under the tested conditions), NT = not tested.*

HsNUDT14 has a similar substrate specificity profile as HsNUDT5. According to literature, also preferentially hydrolyzes ADP-sugars, NADH, and additionally also UDP-glucose (Heyen *et al.*, 2009, Carreras-Puigvert *et al.*, 2017). HsNUDT14 efficiently hydrolyzed five small molecules but showed no detectable activity toward any of the tested capped RNAs. The most efficiently cleaved substrates were Ap_2A (92.3 ± 13.2%) and ADPR (90.4 ± 7.2%), followed by NADH, FAD and Ap_3A (Figure 26).

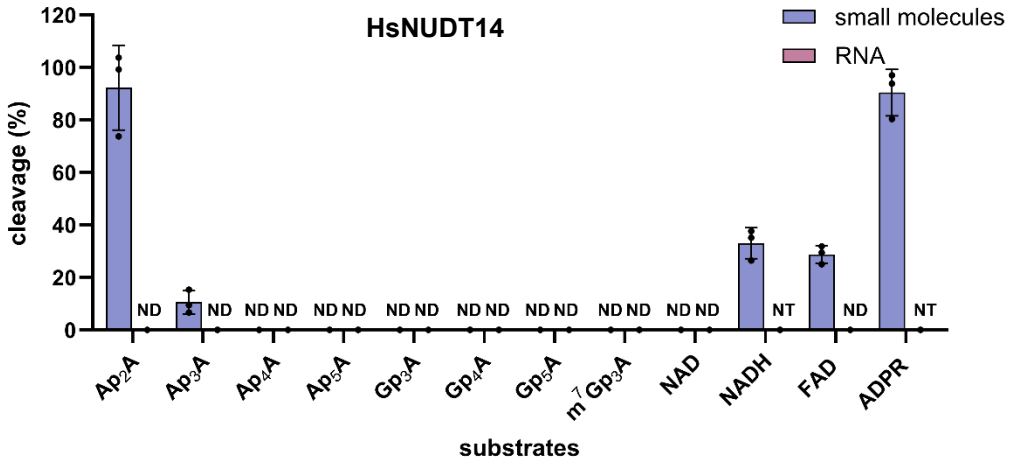

***Figure 26**: Cleavage of small molecules and capped RNAs by HsNUDT14. The graph shows the percentage of substrate hydrolysis by 100 nM HsNUDT14 after 30-minute incubation at 37 °C with 5 µM substrate measured by MGA. Data are presented as mean ± SD from three independent experiments. ND = not detected (cleavage less than 5% observed under the tested conditions), NT = not tested.*

The final enzyme tested, HsNUDT22, is known to hydrolyze UDP-glucose (Carter *et al.*, 2018). This enzyme did not exhibit any detectable hydrolytic activity toward any of the small-molecule or capped RNA substrates under the conditions used in this assay (Figure 27).

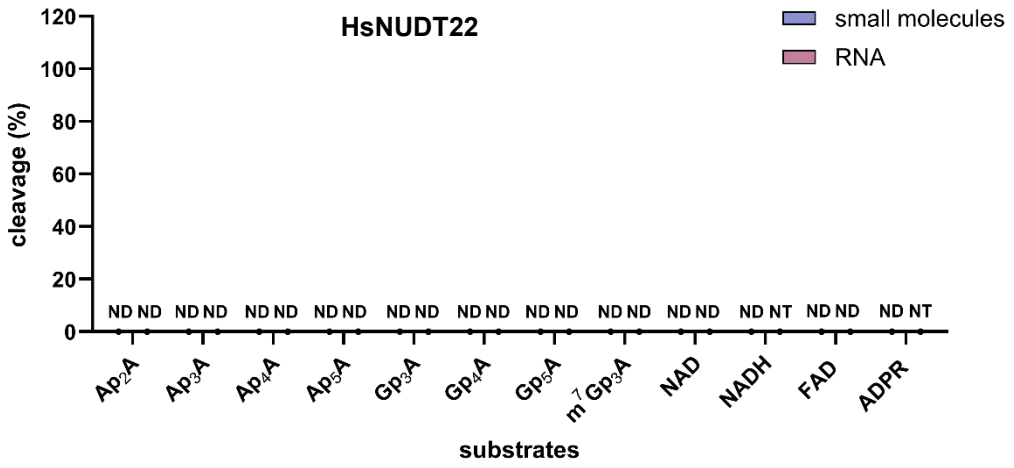

Figure 27*: Cleavage of small molecules and capped RNAs by HsNUDT22. The graph shows the percentage of substrate hydrolysis by 100 nM HsNUDT22 after 30-minute incubation at 37 °C with 5 µM substrate measured by MGA. Data are presented as mean ± SD from three independent experiments. ND = not detected (cleavage less than 5% observed under the tested conditions), NT = not tested.*

5. Discussion

5.1. Production and Purification of MmNUDT12 and RNA Substrates

The study of NudiX enzyme activity required both the availability of active enzymes and the preparation of a set of capped RNA substrates. While most of the enzymes used in this work were obtained through collaboration with Pål Stenmark group at Stockholm University, HsNUDT2 was provided by Potužník *et al.* (2023), and MmNUDT12 was produced as part of this thesis. MmNUDT12 was expressed in *E. coli* BL21 and purified using IMAC, followed by SEC. Despite following an established protocol (Mititelu, 2024), the overall yield of MmNUDT12 was relatively low (0.4 mg). This reduced yield may have been caused by partial protein degradation during expression or handling, or by inefficient binding of the His-tagged protein to the IMAC resin. However, the amount of MmNUDT12 was sufficient for the experiments presented in this thesis.

Following protein preparation, the next crucial step involved the synthesis and purification of capped RNAs, which served as substrates for enzymatic assays with various NudiX enzymes. In total, twelve capped RNAs were synthesized, out of which ten were successfully purified to a purity equal to or higher than 80%. The identity of each capped RNA was confirmed by LC-MS analysis (performed by Dr. Anton Škríba).

Minor impurities typically consisted of RNAs capped with the correct moiety but varying by one nucleotide in length, either shorter or longer than the desired transcript. The longer variations are likely a result of the known tendency of T7 RNA polymerase to add non-templated nucleotides at the 3′ end of transcripts, as previously described (Jain *et al.*, 2020). Importantly, none of these contaminants are expected to significantly affect the enzymatic assays performed in this study.

For nine of the ten RNAs, the observed masses corresponded to the calculated values. However, the Gp_4A-RNA sample showed a mass 16 Da higher than the calculated one, which could correspond either to the incorporation of G instead of A or to the oxidation of G. To investigate the first possibility, Dr. Škríba tested whether the Gp_4A stock solution used for IVT was contaminated with Gp_4G. The results showed that Gp_4A stock solution was 100% clean and excluded the potential contamination. Oxidation of guanosine during handling therefore remains a possible explanation. Still, it is unusual that this shift was observed only in this one

RNA sample. For publication purposes, the identity of the cap needs to be clarified, and the issue resolved.

Two capped RNAs – NADH-RNA and ADPR-RNA – could not be purified to 80% purity or higher. This could be caused by their chemical instability and susceptibility to degradation. In the case of NADH-RNA, exposure to oxidizing conditions leads to the formation of mixed populations of NADH- and NAD-capped RNAs, complicating purification. Although a single peak was collected during HPLC purification, subsequent control run revealed that approximately 30% of the sample has already been oxidized to NAD-RNA. This instability under standard laboratory conditions has been previously reported (Makarov *et al.*, 2021). One potential strategy to mitigate this degradation could involve the addition of higher concentrations of reducing agents during purification. However, such additives may interfere with the MGA (Feng *et al.*, 2011).

In contrast to NADH-RNA, challenges with ADPR-RNA purification were evident already during the HPLC separation. ADPR-RNA consistently co-eluted with p-RNA, and these two RNAs could not be separated despite multiple HPLC gradient optimization attempts. A likely explanation of the presence of p-RNA in the sample is that ADPR-RNA goes through spontaneous degradation under alkaline conditions and at room temperature, resulting in the formation of AMP and ribose-5-phosphate (Iordanov *et al.*, 2016). The presence of p-RNA in the ADPR-RNA sample was further confirmed by LC-MS analysis. Since the p-RNA in the sample would interfere with the MGA by contributing to phosphate signal as a source of P_i after rSAP treatment, this sample could not be used for further enzymatic studies. One potential solution would be to add one more enzymatic step before purification that would selectively degrade the p-RNA by 5'-monophosphate exoribonucleases, such as XRN1 (Johnson and Kolodner, 1991).

5.2. Method Comparison for Evaluating NudiX Enzyme Activity

While MGA has previously been applied to investigate the hydrolysis of small molecules (Carreras-Puigvert *et al.*, 2017), in this study the MGA was also used to evaluate the hydrolysis of capped RNAs, offering a comprehensive comparison of these approaches. Two enzymes – HsNUDT2 and MmNUDT12 – were evaluated using both MGA and the standard PAGE/HPLC analysis.

One of the main advantages of MGA is that it enables the analysis of both small molecules and capped RNAs under identical conditions and at the same substrate concentrations. Furthermore, MGA allows for high-throughput quantification of P_i released during enzymatic hydrolysis, offering a rapid, sensitive, and scalable method for detecting NudiX activity. In contrast, HPLC and PAGE each have methodological limitations that complicate direct comparison between small molecules and RNA cleavage. HPLC, used for small molecules, typically requires higher substrate concentrations in order to reliably quantify its consumption after the reaction. On the other hand, PAGE, used for RNA, employs radioactively labelled RNA, which can be monitored at very low concentrations, but higher amounts would be very laborious and expensive. Therefore, it is difficult to align experimental conditions across these methods.

Another important distinction between the MGA and PAGE approaches lies in the RNA substrates used. For PAGE-based decapping assays, a 35-mer RNA treated with DNase I was used, following the standard protocol of the Hana Cahová Group (Hudeček *et al.*, 2020). However, this 35-mer RNA was not suitable for MGA, as the assay's lower detection limit is approximately 5 μM substrate concentration, which would require producing large quantities of 35-mer RNA by IVT. To address this, a shorter 6-mer RNA was used for MGA experiments. A major advantage of using this short RNA is the ability to purify it using HPLC, allowing for well-defined purity and identity of the capped RNA. Importantly, since the length of the RNA should not influence cap cleavage efficiency, the 6-mer serves as a suitable alternative.

Additionally, the reaction buffer also differed between the two approaches. In our laboratory, the standard reaction buffer used for PAGE and HPLC analysis is the NudC buffer (composition in Materials) (Hudeček *et al.*, 2020). However, MGA was previously established using NudiX reaction buffer (composition in Materials) (Carreras-Puigvert *et al.*, 2017). Since HsNUDT5 showed no detectable activity in the NudC buffer but was active in the NudiX buffer, the NudiX buffer was used for all MGA experiments to ensure consistency and comparability across all tested enzymes.

The main objective of this study was to systematically evaluate the substrate specificity of selected NudiX enzymes using the MGA and to validate these findings by comparison with standard analytical techniques: PAGE and HPLC. This comparison was performed for two enzymes: HsNUDT2 and MmNUDT12.

HsNUDT2, a well-characterized member of the NudiX superfamily, is known for its ability to hydrolyze Np_nNs, particularly Ap_4A (McLennan, 2006). In this study, a panel of small molecules and their corresponding capped RNAs was tested using both MGA and HPLC/PAGE. Both approaches consistently demonstrated that HsNUDT2 predominantly cleaves Ap_4A, Ap_5A, Gp_4A, Gp_5A, and their corresponding RNAs (Ap_4A-RNA, Ap_5A-RNA, Gp_4A-RNA, and Gp_5A-RNA). However, additional cleavage of Gp_3A-RNA was observed only in the PAGE analysis. Although both methods used buffers adjusted to the same pH and containing Mg^{2+} as a cofactor, subtle differences in buffer composition may have influenced enzyme activity or substrate recognition. Another factor that could affect the outcome of the screening is the concentration of the substrates used. For PAGE analysis, 100 ng of RNA was loaded, corresponding to approximately 0.008 nmol, whereas for MGA, 0.1 nmol of RNA was used. These differences in substrate concentration could potentially affect the reaction kinetics and detection of cleavage by HsNUDT2. For instance, HsNUDT2 cleaves approximately 50% of Gp_3A-RNA in the PAGE analysis, corresponding to around 0.004 nmol. Even if the enzyme kinetic was independent of substrate concentration, the cleavage detected by MGA would represent 0.004 nmol out of 0.1 nmol and would therefore be undetectable.

For MmNUDT12, PAGE and HPLC were used primarily to confirm the enzymatic activity of the purified recombinant enzyme rather than to perform a full substrate screen. Therefore, only three small molecules and their corresponding capped RNAs were tested using these methods. Despite differences in buffer composition and substrate concentrations (as discussed above), the results obtained by MGA and PAGE/HPLC were consistent, supporting the reliability of MGA as a screening method.

5.3. Substrate Specificity of Mammalian NudiX enzymes

Many studies have investigated the substrate specificity of NudiX enzymes, often describing their ability to hydrolyze a broad spectrum of nucleotide-derived small molecules (McLennan, 2006; Carreras-Puigvert *et al.*, 2017). More recently, increasing attention has focused on their RNA decapping activity, particularly toward non-canonical RNA caps such as NAD, FAD, and Np_nNs (Grudzien-Nogalska *et al.*, 2019; Sharma *et al.*, 2020; Potužník *et al.*, 2023). However, no direct comparison has yet been made between the enzymatic activity toward small molecules and their corresponding RNA caps. Moreover, these enzymes have not been

systematically studied for their RNA decapping activity, and their substrate preferences toward RNA caps therefore remain unexplored.

The observed specificity of HsNUDT2 for Np_nNs with $n \geq 4$ is consistent with previous findings (McLennan, 2006; Carreras-Puigvert *et al.*, 2017). Moreover, the ability of HsNUDT2 to hydrolyze Ap_4A-RNA and other Np_nN-RNAs (where n = 4, 5) both in vitro and in vivo, has been previously demonstrated (Potužník *et al.*, 2023), and was further confirmed in this study. In addition to my results, mammalian NUDT2 was also shown to cleave FAD-RNA, Gp_3N-RNA and m^7Gp_3N-RNA in vitro (Sharma *et al.*, 2020). The cleavage of m^7G-capped RNA was also confirmed by Husain et al. (2024). However, these results were not observed in this study.

In a comprehensive study of substrate specificity of human NudiX enzymes toward small molecules (Carreras-Puigvert *et al.*, 2017), NUDT12 was shown to cleave a broad range of substrates including NADH, NAD, ADPR, and Ap_nAs. However, its activities toward free m^7Gp_3A and Gp_3A have not been previously tested. This study demonstrates strong hydrolysis (69.8 ± 3.6%) of Gp_3A and a weak activity (10.3 ± 2.2%) toward m^7Gp_3A, revealing new substrates of MmNUDT12. Sharma *et al*., (2020) showed that mammalian NUDT12 has RNA decapping activity toward m^7Gp_3A-RNA and Gp_3A-RNA, which was not confirmed in this study. The fact that mammalian NUDT12 cleaves Ap_nA-RNAs has not been previously reported and was first described in this study. This finding will be part of a manuscript currently under revision describing the newly discovered Ap_2N-RNA, to which my results contributed by identifying NUDT12 as a potential decapping enzyme for this structure. Finally, MmNUDT12 showed no activity toward FAD-RNA, consistent with Sharma *et al.*, (2020).

NUDT1 and NUDT15 exhibited similar substrate specificity. Both were active toward dGTP, consistent with previous findings (Carreras-Puigvert *et al.*, 2017). Given their known triphosphatase activity, their ability to hydrolyze ATP and ppp-RNA was also evaluated. None of these substrates were cleaved by these enzymes. For NUDT15, lack of activity toward ppp-RNA is consistent with earlier observations (Laudenbach *et al.*, 2021), while for NUDT1, this study represents the first test of such activity. These two enzymes have been reported not to cleave ATP, and this result was confirmed in this study as well. Notably, NUDT1 and NUDT15 belong to the same structural subfamily, which may explain their overlapping substrate preferences (Carreras-Puigvert *et al.*, 2017).

NUDT5 and NUDT14 displayed similar substrate specificity. None of them exhibited RNA decapping activity, consistent with Sharma *et al.* (2020), and both efficiently hydrolyzed ADP-ribose, which is considered their primary substrate (Carreras-Puigvert *et al.*, 2017). Both enzymes also cleaved Ap_2A and FAD. While activity of NUDT5 toward these small molecules was previously observed (Yang *et al.*, 2000), the activity of NUDT14 toward Ap_2A and FAD was not directly examined before, making this a novel finding. Additionally, both enzymes cleaved NADH, consistent with Carreras-Puigvert *et al.* (2017). According to structural analysis, NUDT5 and NUDT14 also belong to the same NudiX subfamily (Carreras-Puigvert *et al.*, 2017), supporting the observed similarities in substrate specificity.

Carter *et al.* (2018) described NUDT22 as a very specific NudiX enzyme with a unique protein fold and specific substrate specificity toward UDP-glucose and UDP-galactose. These substrates were not available for testing in this study, making it impossible to verify the activity of this enzyme. Therefore, this experiment will need to be done in the future. The lack of activity toward any other tested substrates is consistent with literature.

Finally, the m^7G-capped RNA decapping activity previously reported for NUDT2, NUDT12, and NUDT15 (Sharma *et al.*, 2020) was not observed in our study. To address this issue, the reactions were repeated using the exact same buffer composition as reported by Sharma *et al.* (2020) – the NudC buffer (composition in Materials) supplemented with 0.5 mM $MnCl_2$. However, we did not observe cleavage of m^7G-capped RNA by any of the three enzymes under these conditions (data not shown). This result further highlights the possibility that enzyme activity may depend on experimental variables, such as substrate preparation, or enzyme batch variability.

6. Conclusions

This thesis systematically investigated the substrate specificity of seven selected mammalian NudiX enzymes, with a particular focus on non-canonically capped RNAs. The work included the successful expression and purification of MmNUDT12 enzyme and the synthesis and purification of a set of capped 6-mer RNAs. These RNAs were produced with purity equaled to or higher than 80% and with defined cap structures, making them suitable for enzymatic assays.

Two complementary approaches were employed to characterize NudiX enzymatic activity: standard analytical methods (PAGE and HPLC) and MGA. MGA proved to be a reliable, high-throughput method for detecting phosphate release during the enzymatic reaction and allowed for the direct comparison of small molecule and RNA substrates under identical reaction conditions. Validation using PAGE and HPLC confirmed the accuracy of MGA results for HsNUDT2 and MmNUDT12. MGA represents the first assay of its kind applicable to both small molecules and RNA substrates and will serve as a valuable tool for studying other decapping enzymes in our laboratory in the future.

The enzymatic screening revealed preferred substrates for each NudiX enzyme. While the results largely align with previously published data, some deviations or novel substrates were observed, highlighting the influence of reaction conditions, buffer composition, and substrate concentration on enzyme behavior. Notably, HsNUDT5, MmNUDT12, and HsNUDT14 demonstrated a clear preference for small molecules, whereas HsNUDT2 preferentially hydrolyzed RNA substrates over small molecules. This finding highlights that HsNUDT2 is the only tested enzyme that preferentially acts as RNA decapping enzyme preferably hydrolyzing Ap_4A-RNA and Ap_5A-RNA. Additionally, MmNUDT12 was shown to cleave Ap_2A-RNA and Ap_2G-RNA. This novel finding is included in a publication which is currently under review.

Overall, this study expands the current understanding of mammalian NudiX substrate preferences and demonstrates the value of MGA as a powerful tool for enzymatic characterization. These findings contribute to a more comprehensive understanding of RNA decapping mechanisms.

7. References

Abdelraheim, S.R., Spiller, D.G. and McLennan, A.G. (2003) 'Mammalian NADH diphosphatases of the Nudix family: cloning and characterization of the human peroxisomal NUDT12 protein', *Biochemical Journal*, 374(Pt 2):329.

Avalos, J.L., Bever, K.M. and Wolberger, C. (2005) 'Mechanism of sirtuin inhibition by nicotinamide: altering the NAD(+) cosubstrate specificity of a Sir2 enzyme', *Molecular cell*, 17(6):855–868.

Baykov, A.A., Evtushenko, O.A. and Avaeva, S.M. (1988) 'A malachite green procedure for orthophosphate determination and its use in alkaline phosphatase-based enzyme immunoassay', *Analytical Biochemistry*, 171(2):266–270.

Benoni, B. *et al.* (2022) 'HIV–1 infection reduces NAD capping of host cell snRNA and snoRNA', *ACS Chemical Biology*, 19(6):1243-1249.

Bessman, M.J., Frick, D.N. and O'handley, S.F. (1996) 'The MutT Proteins or "Nudix" Hydrolases, a Family of Versatile, Widely Distributed, "Housecleaning" Enzymes*', *Journal of Biological Chemistry*, 271(41):25059-62.

Bird, J.G. *et al.* (2016) 'The mechanism of RNA 5′ capping with NAD^+, NADH and desphospho-CoA', *Nature*, 535(7612):444-7.

Bruce Alberts *et al.* (2015) 'Molecular Biology of the Cell, Sixth Edition', *International Journal of Molecular Sciences*, (12):1–1464.

Cahová, H. *et al.* (2015) 'NAD captureSeq indicates NAD as a bacterial cap for a subset of regulatory RNAs', *Nature*, 519(7543):374–377.

Cappannini, A. *et al.* (2024) 'MODOMICS: a database of RNA modifications and related information. 2023 update', *Nucleic Acids Research*, 52(D1):239–244.

Carreras-Puigvert, J. *et al.* (2017) 'A comprehensive structural, biochemical and biological profiling of the human NUDIX hydrolase family', *Nature Communications*, 8(1):1541.

Carrington, J.C. and Ambros, V. (2003) 'Role of microRNAs in plant and animal development', *Science*, 301(5631):336–338.

Carter, M. *et al.* (2015) 'Crystal structure, biochemical and cellular activities demonstrate separate functions of MTH1 and MTH2', *Nature Communications*, 6:7871.

Carter, M. *et al.* (2018) 'Human NUDT22 Is a UDP-Glucose/Galactose Hydrolase Exhibiting a Unique Structural Fold', *Structure (London, England : 1993)*, 26(2):295-303.

Carthew, R.W. and Sontheimer, E.J. (2009) 'Origins and Mechanisms of miRNAs and siRNAs', *Cell*, 136(4):642–655.

Chambon, P., Weill, J.N. and Mandel, P. (1963) 'Nicotinamide mononucleotide activation of new DNA-dependent polyadenylic acid synthesizing nuclear enzyme', *Biochemical and Biophysical Research Communications*, 11(1):39-43.

Chen, K. and Rajewsky, N. (2007) 'The evolution of gene regulation by transcription factors and microRNAs*', *Nature Reviews Genetics*, 8(2):93–103.

Chow, L.T. *et al.* (1977) 'An amazing sequence arrangement at the 5' ends of adenovirus 2 messenger RNA', *Cell*, 12(1):1–8.

Cohn, W.E. and Volkin, E. (1951) 'Nucleoside-5′-Phosphates from Ribonucleic Acid', *Nature*, 167(4247):483–484.

Deana, A., Celesnik, H. and Belasco, J.G. (2008) 'The bacterial enzyme RppH triggers messenger RNA degradation by 59 pyrophosphate removal', *Nature*, 451(7176):355-8.

Debar, L. *et al.* (2023) 'NUDT6 and NUDT9, two mitochondrial members of the NUDIX family, have distinct hydrolysis activities', *Mitochondrion*, 71:93–103.

Deng, X. *et al.* (2023) 'The roles and implications of RNA m6A modification in cancer*', *Nature Reviews Clinical Oncology 2023 20:8*, 20(8):507–526.

Feng, J. *et al.* (2011) 'An improved malachite green assay of phosphate: mechanism and application', *Analytical biochemistry*, 409(1):144–149.

Fire, A. *et al.* (1998) 'Potent and specific genetic interference by double-stranded RNA in Caenorhabditis elegans', *Nature*, 391(6669):806–811.

Franco, M.K. and Koutmou, K.S. (2022) 'Chemical modifications to mRNA nucleobases impact translation elongation and termination', *Biophysical Chemistry*, 285:106780. .

Frindert, J. *et al.* (2018) 'Identification, Biosynthesis, and Decapping of NAD-Capped RNAs in B. subtilis*', *Cell Reports*, 24(7):1890-1901.

Furuichi, Y., Lafiandra, A. and Shatkin, A.J. (1977) '5'-Terminal structure and mRNA stability', *Nature*, 266(5599):235-9.

Ghildiyal, M. and Zamore, P.D. (2009) 'Small silencing RNAs: an expanding universe*', *Nature Reviews Genetics*, 10(2):94-108.

Giammarinaro, P.I. *et al.* (2022) 'Diadenosine tetraphosphate regulates biosynthesis of GTP in Bacillus subtilis', *Nature Microbiology*, 7(9), pp. 1442–1452.

Gomes-Filho, J.V. *et al.* (2023) 'Identification of NAD-RNA species and ADPR-RNA decapping in Archaea', *Nature Communications*, 14(1):7597.

Götz, K.H. *et al.* (2019) 'Formation of the Alarmones Diadenosine Triphosphate and Tetraphosphate by Ubiquitin- and Ubiquitin-like-Activating Enzymes', *Cell Chemical Biology*, 26(11):1535-1543

Grace Chen, Y. *et al.* (2009) 'LC/MS analysis of cellular RNA reveals NAD-linked RNA', *Nature Chemical Biology*, 5(12):879-81.

Grudzien-Nogalska, E. *et al.* (2016) 'Nudt3 is an mRNA decapping enzyme that modulates cell migration', *RNA*, 22(5):773-81.

Grudzien-Nogalska, E. *et al.* (2019) 'Structural and mechanistic basis of mammalian Nudt12 RNA deNADding', *Nature Chemical Biology*, 15(6):575-582.

Heyen, C.A. *et al.* (2009) "Characterization of mouse UDP-glucose pyrophosphatase, a Nudix hydrolase encoded by the Nudt14 gene," *Biochemical and biophysical research communications*, 390(4):1414–1418.

Hilderman, R.H. and Ortwerth, B.J. (1987) ‘A preferential role for lysyl-tRNA4 in the synthesis of diadenosine 5’,5’’’-P1,P4-tetraphosphate by an arginyl-tRNA synthetase-lysyl-tRNA synthetase complex from rat liver’, *Biochemistry*, 26(6):1586–1591.

Höfer, K. *et al.* (2016) ‘Structure and function of the bacterial decapping enzyme NudC’, *Nature Chemical Biology*, 12(9):730-4.

Huang, F. (2003) ‘Efficient incorporation of CoA, NAD and FAD into RNA by in vitro transcription’, *Nucleic Acids Research*, 31(3):e8.

Hudeček, O. *et al.* (2020) ‘Dinucleoside polyphosphates act as 5′-RNA caps in bacteria’, *Nature Communications*, 11(1):1052.

Hurtig, J.E. and Van Hoof, A. (2022) ‘Yeast Dxo1 is required for 25S rRNA maturation and acts as a transcriptome-wide distributive exonuclease’, *RNA*, 28(5):657-667.

Husain, R.A. *et al.* (2024) ‘Biallelic NUDT2 variants defective in mRNA decapping cause a neurodevelopmental disease’, *Brain : a journal of neurology*, 147(4):1197–1205.

Iordanov, I. *et al.* (2016) ‘The proposed channel-enzyme transient receptor potential melastatin 2 does not possess ADP ribose hydrolase activity’, *eLife*, 5:e17600.

Jain, N. *et al.* (2020) ‘Transcription polymerase-catalyzed emergence of novel RNA replicons’, *Science*, 368(6487).

Jiao, X. *et al.* (2010) ‘Identification of a quality-control mechanism for mRNA 5’-end capping’, *Nature*, 467(7315):608-11.

Jiao, X. *et al.* (2013) ‘A Mammalian Pre-mRNA 5′ End Capping Quality Control Mechanism and an Unexpected Link of Capping to Pre-mRNA Processing’, *Molecular Cell*, 50(1):104–115.

Jiao, X. *et al.* (2017) ‘5′ End Nicotinamide Adenine Dinucleotide Cap in Human Cells Promotes RNA Decay through DXO-Mediated deNADding’, *Cell*, 168(6):1015-1027.

Johnson, A.W. and Kolodner, R.D. (1991) ‘Strand exchange protein 1 from Saccharomyces cerevisiae. A novel multifunctional protein that contains DNA strand exchange and exonuclease activities’, *Journal of Biological Chemistry*, 266(21):14046–14054.

Kago, G. and Parrishid, S. (2021) ‘The Mimivirus L375 Nudix enzyme hydrolyzes the 5’ mRNA cap’, *PLOS One*, 16(9):e0245820.

Kerr, E.W., Shumar, S.A. and Leonardi, R. (2019) ‘Nudt8 is a novel CoA diphosphohydrolase that resides in the mitochondria’, *FEBS letters*, 593(11):1133–1143.

Kisselev, L.L. *et al.* (1998) ‘Diadenosine oligophosphates (Ap(n)A), a novel class of signalling molecules?’, *FEBS letters*, 427(2):157–163.

Kowtoniuk, W.E. *et al.* (2009) ‘A chemical screen for biological small molecule-RNA conjugates reveals CoA-linked RNA’, *Proceedings of the National Academy of Sciences of the United States of America*, 106(19):7768–7773.

Kramer, S. (2017) ‘The ApaH-like phosphatase TbALPH1 is the major mRNA decapping enzyme of trypanosomes’, *PLOS Pathogens*, 13(6):e1006456.

Kramer, S. and McLennan, A.G. (2019) ‘The complex enzymology of mRNA decapping: Enzymes of four classes cleave pyrophosphate bonds*’, *Wiley Interdisciplinary Reviews: RNA*, 10(1):e1511.

Langelier, M.F. *et al.* (2018) ‘NAD+ analog reveals PARP-1 substrate-blocking mechanism and allosteric communication from catalytic center to DNA-binding domains’, *Nature Communications*, 9(1):844.

Laudenbach, B.T. *et al.* (2021) ‘NUDT2 initiates viral RNA degradation by removal of 5’-phosphates’, *Nature communications*, 12(1):6918.

Lee, P.C., Bochner, B.R. and Ames, B.N. (1983) ‘Diadenosine 5’,5’"-P1,P4-tetraphosphate and Related Adenylylated Nucleotides in Salmonella typhimurium"’, *The Journal of Biological Chemistry*, 258(11):6827–6834.

Löcherer, C. *et al.* (2022) ‘Staphylococcus aureus Small RNAs Possess Dephospho-CoA 5-Caps, but No CoAlation Marks’, *Noncoding RNA*, 8(4):46.

Luciano, D.J., Levenson-Palmer, R. and Belasco, J.G. (2019) 'Stresses that Raise Np4A Levels Induce Protective Nucleoside Tetraphosphate Capping of Bacterial RNA', *Molecular Cell*, 75(5):957-966.

Maciej, V.D. and Chakrabarti, S. (2022) 'One enzyme, many substrates: How the vaccinia virus enzyme D9 decaps host and viral mRNAs alike', *Structure*, 30(5):653–654.

Makarov, M. V. *et al.* (2021) 'Chemical and Biochemical Reactivity of the Reduced Forms of Nicotinamide Riboside', *ACS Chemical Biology*, 16(4):604–614.

Maki, H. and Sekiguchi, M. (1992) 'MutT protein specifically hydrolyses a potent mutagenic substrate for DNA synthesis', *Nature*, 355(6357):273–275.

McCown, P.J. *et al.* (2020) 'Naturally occurring modified ribonucleosides*', *Wiley Interdisciplinary Reviews. RNA*, 11(5):e1595.

McLennan, A.G. (1999) 'The MutT motif family of nucleotide phosphohydrolases in man and human pathogens*', *International Journal of Molecular Medicine*, 4(1):79–89.

McLennan, A.G. (2006) 'The Nudix hydrolase superfamily*', *Cellular and Molecular Life Sciences*, 63(2):123–143.

Miras-Portugal, M.T., Gualix, J. and Pintor, J. (1998) 'The neurotransmitter role of diadenosine polyphosphates', *FEBS letters*, 430(1–2):78–82.

Mititelu, M.-B. *et al.* (2023) 'Arabidopsis thaliana NudiXes have RNA-decapping activity', *RSC Chemical Biology*, 4:223.

Mititelu, M.-B. (2024) 'New types of RNA non-canonical caps and their degradation by NudiX enzymes'. Dizertační práce, Univerzita Karlova, Praha.

Munir, A., Banerjee, A. and Shuman, S. (2018) 'NAD^+-dependent synthesis of a 5-phospho-ADP-ribosylated RNA/DNA cap by RNA 2-phosphotransferase Tpt1', *Nucleic Acids Research*, 46(18):9617–9624.

Muthukrishnan, S. *et al.* (1975) '5'-Terminal 7-methylguanosine in eukaryotic mRNA is required for translation', *Nature*, 255(5503):33–37.

Parrish, S., Resch, W. and Moss, B. (2007) 'Vaccinia virus D10 protein has mRNA decapping activity, providing a mechanism for control of host and viral gene expression', *Proceedings of the National Academy of Sciences of the United States of America*, 104(7):2139–2144.

Ponting, C.P., Oliver, P.L. and Reik, W. (2009) 'Evolution and functions of long noncoding RNAs', *Cell*, 136(4):629–641.

Potužník, J.F. *et al.* (2023) 'Diadenosine Tetraphosphate (Ap4A) Serves as a 5' RNA Cap in Mammalian Cells', *Angewandte Chemie*, 63(6):e202314951.

Potužník, J.F. and Cahova, H. (2024) 'If the 5' cap fits (wear it)–Non-canonical RNA capping*', *RNA Biology*, 21(1):1–13.

Quintas, A. *et al.* (2017) 'Characterization of the African Swine Fever Virus Decapping Enzyme during Infection*', *Journal of Virology*, 91(24):e00990-17.

Ramanathan, A., Robb, G.B. and Chan, S.-H. (2016) 'mRNA capping: biological functions and applications*', *Nucleic Acids Research*, 44(16):7511–7526.

Rapaport, E. and Zamecnik, P.C. (1976) 'Presence of diadenosine 5',5''' -P1, P4-tetraphosphate (Ap4A) in mamalian cells in levels varying widely with proliferative activity of the tissue: a possible positive "pleiotypic activator".', *Proceedings of the National Academy of Sciences*, 73(11):3984–3988.

Sapkota, K. *et al.* (2024) 'Post-transcriptional capping generates coenzyme A-linked RNA', *RNA Biology*, 21(1):44–55.

Schlüter, H. *et al.* (1998) 'Adenosine(5') oligophospho-(5') guanosines and guanosine(5') oligophospho-(5') guanosines in human platelets', *The Journal of Clinical Investigation*, 101(3):682–688.

Schreiber, V. *et al.* (2006) 'Poly(ADP-ribose): novel functions for an old molecule*', *Nature Reviews Molecular Cell Biology*, 7(7):517-28.

Sharma, S. *et al.* (2020) 'Mammalian Nudix proteins cleave nucleotide metabolite caps on RNAs', *Nucleic Acids Research*, 48(12):6788–6798.

Shatkin, A.J. and Manley, J.L. (2000) 'The ends of the affair: Capping and polyadenylation*', *Nature Structural Biology*, 7(10):838-42.

She, M. *et al.* (2005) 'Crystal structure and functional analysis of Dcp2p from Schizosaccharomyces pombe', *Nature Structural & Molecular Biology*, 13(1):63–70.

Sherwood, A. V *et al.* (2023) 'Hepatitis C virus RNA is 5′-capped with flavin adenine dinucleotide', *Nature*, 619(7971):811-818.

Sheth, U. and Parker, R. (2003) 'Decapping and decay of messenger RNA occur in cytoplasmic processing bodies', *Science (New York, N.Y.)*, 300(5620):805–808.

Shumar, S.A. *et al.* (2018) 'Nudt19 is a renal CoA diphosphohydrolase with biochemical and regulatory properties that are distinct from the hepatic Nudt7 isoform', *The Journal of biological chemistry*, 293(11):4134–4148.

Song, M.-G., Bail, S. and Kiledjian, M. (2013) 'Multiple Nudix family proteins possess mRNA decapping activity', *RNA*, 19(3):390-9.

Takagi, Y. *et al.* (2012) 'Human MTH3 (NUDT18) Protein Hydrolyzes Oxidized Forms of Guanosine and Deoxyguanosine Diphosphates', *Journal of Biological Chemistry*, 287:21541–21549.

Tashiro, K. *et al.* (2023) 'Chemoenzymatic and Synthetic Approaches To Investigate Aspartate- and Glutamate-ADP-Ribosylation', *Journal of the American Chemical Society*, 145(25):14000–14009.

Varshavsky, A. (1983) 'Diadenosine 5′, 5‴-P1, P4-tetraphosphate: a pleiotropically acting alarmone?', *Cell*, 34(3):711–712.

Walters, R.W. *et al.* (2017) 'Identification of NAD+ capped mRNAs in Saccharomyces cerevisiae', *Proceedings of the National Academy of Sciences of the United States of America*, 114(3):480–485.

Wang, Y. *et al.* (2019) 'NAD$^+$-capped RNAs are widespread in the Arabidopsis transcriptome and can probably be translated', *Proceedings of the National Academy of Sciences of the United States of America*, 116(24):12094–12102.

Wang, J. *et al.* (2019) ‘Quantifying the RNA cap epitranscriptome reveals novel caps in cellular and viral RNA’, *Nucleic Acids Research*, 47(2):130.

Weixler, L. *et al.* (2021) ‘ADP-ribosylation of RNA and DNA: from in vitro characterization to in vivo function’, *Nucleic Acids Research*, 49(7):3634–3650.

Weixler, L., Feijs, K.L.H. and Zaja, R. (2022) ‘ADP-ribosylation of RNA in mammalian cells is mediated by TRPT1 and multiple PARPs’, *Nucleic Acids Research*, 50(16):9426–9441.

Werner, M. *et al.* (2011) ‘2’-O-ribose methylation of cap2 in human: function and evolution in a horizontally mobile family*’, *Nucleic acids research*, 39(11):4756–4768.

Westheimer F.H. (1986) ‘Polyribonucleic acids as enzymes’, *Nature*, 319(6054):534-5.

Wolfram-Schauerte, M. *et al.* (2023) ‘A viral ADP-ribosyltransferase attaches RNA chains to host proteins’, *Nature*, 620(7976):1054-1062.

Xiang, S. *et al.* (2009) ‘Structure and function of the 59R39 exoribonuclease Rat1 and its activating partner Rai1’, *Nature,* 458(7239):784-8.

Xu, J. *et al.* (2006) ‘Arabidopsis DCP2, DCP1, and VARICOSE form a decapping complex required for postembryonic development’, *The Plant Cell*, 18(12):3386–3398.

Yamada-Okabe, T. *et al.* (1998) ‘Isolation and characterization of a human cDNA for mRNA 5’-capping enzyme’, *Nucleic Acids Research*, 26(7):1700.

Yang, H. *et al.* (2000) ‘Cloning and Characterization of a New Member of the Nudix Hydrolases from Human and Mouse’, *Journal of Biological Chemistry*, 275:8844–8853.

Yoshimura, K. and Shigeoka, S. (2014) ‘Versatile physiological functions of the Nudix hydrolase family in Arabidopsis*’, *Bioscience, Biotechnology, and Biochemistry*, 79(3):354-66.

Yu, J. *et al.* (2019) ‘Second messenger Ap4A polymerizes target protein HINT1 to transduce signals in FcεRI-activated mast cells’, *Nature Communications*, 10(1):1–12.

Zamecnik, P.G. *et al.* (1966) ‘Enzymatic synthesis of diadenosine tetraphosphate and diadenosine triphosphate with a purified lysyl-sRNA synthetase’, *Biochemical and Biophysical Research Communications*, 24(1):91–97.

Zhang, Y. *et al.* (2020) ‘Extensive 5′-surveillance guards against non-canonical NAD-caps of nuclear mRNAs in yeast’, *Nature Communications*, 11(1):5508.